

# **CORROSION OF SIMFUEL IN AERATED CARBONATE SOLUTION CONTAINING CALCIUM AND SILICATE**

*Prepared for*

**U.S. Nuclear Regulatory Commission  
Contract NRC-02-07-006**

*Prepared by*

**H. Jung<sup>1</sup>**

**T. Ahn<sup>2</sup>**

**K. Axler<sup>1</sup>**

**R. Pabalan<sup>1</sup>**

**D. Pickett<sup>1</sup>**

**<sup>1</sup>Center for Nuclear Waste Regulatory Analyses  
San Antonio, Texas**

**<sup>2</sup>U.S. Nuclear Regulatory Commission  
Washington, DC**

**September 2011**

## ABSTRACT

This report documents the results of a previously unpublished set of experiments that evaluated the corrosion behavior of simulated spent nuclear fuel (SIMFUEL) in a high-level radioactive waste repository disposal environment. The purpose of the experiments is to confirm a range of dissolution rates of spent nuclear fuel (SNF) in a repository relevant environment, specifically under oxidizing conditions, and to assess a potential effect of radionuclide sorption onto the oxides formed on stainless steel. Specific environmental factors are represented by exposure, at room temperature, of the SIMFUEL to aerated solutions of NaCl+NaHCO<sub>3</sub> with and without calcium and silicate addition to simulate a groundwater or in-package chemistry water in a repository environment. Two SIMFUEL compositions were studied, representing SNF with 3 or 6 percent burnups. For the sorption test, a stainless steel disk was immersed in the posttest solutions and the concentrations of dissolved metallic species were compared to those in the posttest solutions without stainless steel.

For all tested cases, the corrosion potentials of SIMFUEL increased with time and reached a steady state in a range of 0.06 to 0.12 V<sub>SCE</sub> within 72 hours. With immersion time, the polarization resistance increased at the corrosion potential, indicating possible blocking effects due to accumulation of corrosion products on the SIMFUEL electrode. The constructed potential-pH diagram predicts formation of schoepite (UO<sub>3</sub>·2H<sub>2</sub>O), which may support an observation of increased corrosion resistance with time due to secondary phase formation. The addition of calcium and silicate was not measureable in the values of the impedance of polarization resistance measured at the corrosion potential. The impedance with calcium and silicate addition was similar to the case without these ions, indicating relatively minor effects of calcium and silicate in this study up to concentrations of 6.1 and  $1.3 \times 10^{-4}$  M, respectively, on oxidation and dissolution rate of SIMFUEL. The dissolution (corrosion) rate estimated by applying both the Stern-Geary equation and Faraday's law ranged from 1 to 3 mg/m<sup>2</sup> day, which is a range of dissolution rates of SIMFUEL or SNF tested under similar conditions in the literature. A high burnup of SIMFUEL (6 percent) presented a higher dissolution rate than the 3 percent burnup of SIMFUEL under the test conditions in this study.

The results of solution analysis revealed that uranium was a dominant species dissolved in the posttest solutions and the converted dissolution rates based on uranium concentration were consistent with the results of dissolution rates obtained from impedance measurements. Other fission elements, such as barium, molybdenum, strontium, and zirconium, were also dissolved from the SIMFUEL electrode at a relatively high rate. Sorption test results showed that the uranium concentrations in the posttest solutions with a stainless steel disk decreased about 20 percent after 21 days' immersion of stainless steel compared to the concentrations without stainless steel immersed, indicating significant sorption of uranium onto the oxide formed on the stainless steel.

The electrochemical impedance technique was found to be an effective tool in measuring the uranium dissolution rate in real time. This technique can also be used to provide a better understanding of the uranium dissolution process at the interface between uranium oxide and solution. The SIMFUEL characterization results indicate that SIMFUEL can be used as an alternative material to represent the SNF dissolution rate after a long-term containment period when gamma/beta radiation decreases significantly in a repository environment.

# CONTENTS

Section	Page
ABSTRACT .....	ii
FIGURES .....	iv
TABLES .....	v
ACKNOWLEDGMENTS .....	vi
1 INTRODUCTION .....	1-1
1.1 Background Information .....	1-1
1.2 Objective and Scope .....	1-6
2 EXPERIMENTAL DETAILS .....	2-1
2.1 Materials .....	2-1
2.2 Test Solutions .....	2-1
2.3 Test Procedures .....	2-1
3 RESULTS AND DISCUSSION .....	3-1
3.1 SIMFUEL Characterization .....	3-1
3.1.1 Microstructure .....	3-1
3.1.2 Chemical Composition .....	3-1
3.2 Electrochemical Testing .....	3-7
3.2.1 Corrosion Potential Versus Time .....	3-7
3.2.2 Electrochemical Impedance Spectroscopy .....	3-9
3.2.3 Dissolution Rate Estimate .....	3-11
3.3 Solution Chemistry Analyses .....	3-16
3.4 Thermodynamic Stability of Uranium-Simulated Groundwater System at 22 °C [72 °F] .....	3-20
4 CONCLUSIONS .....	4-1
5 REFERENCES .....	5-1

## FIGURES

Figure	Page
1-1 Comparison of Dissolution Rate of Metallic Waste Form at (o) 50 °C (□) 70 °C And (◇) 90 °C With Rates From HLW Glass Model.....	1-5
2-1 Experimental Setup for Electrochemical Test .....	2-2
2-2 Experimental Setup for Sorption Test .....	2-3
3-1 Optical Micrographs of SIMFUEL Surfaces: (a) 3 Percent Burnup and (b) 6 Percent Burnup .....	3-2
3-2 Backscattered Electron Micrographs of SIMFUEL Surfaces: (a) 3 Percent Burnup and (b) 6 Percent Burnup .....	3-3
3-3 Energy Dispersive Spectra of 3 Percent Burnup SIMFUEL: (a) Overall Surface and (b) Grain Boundary Precipitates.....	3-5
3-4 Energy Dispersive Spectra of 6 Percent Burnup SIMFUEL: (a) Overall Surface and (b) Grain Boundary Precipitates.....	3-6
3-5 Corrosion Potential Changes of 3 Percent Burnup SIMFUEL Electrode With Time in a Simulated Groundwater Without (●) and With (Δ) Calcium and Silicate Addition At 22 °C [72 °F].....	3-8
3-6 Corrosion Potential Changes of 6 Percent Burnup SIMFUEL Electrode With Time in a Simulated Groundwater Without (●) and With (Δ) Calcium and Silicate Addition At 22 °C [72 °F].....	3-9
3-7 Electrochemical Impedance Spectra of 3 Percent Burnup SIMFUEL Measured After 24 (●) and 77 Hours (Δ) Immersion at Corrosion Potential Tested in a Simulated Groundwater Without Calcium and Silicate Addition at 22 °C [72 °F] .....	3-10
3-8 Electrochemical Impedance Spectra of 3 Percent Burnup SIMFUEL Measured After 24 (●) and 77 Hours (Δ) Immersion at Corrosion Potential Tested in a Simulated Groundwater With Calcium and Silicate Addition at 22 °C [72 °F] .....	3-12
3-9 Electrochemical Impedance Spectra of 6 Percent Burnup SIMFUEL Measured After 24 (●) and 77 Hours (Δ) Immersion at Corrosion Potential Tested in a Simulated Groundwater Without Calcium and Silicate Addition at 22 °C [72 °F] .....	3-13
3-10 Electrochemical Impedance Spectra of 6 Percent Burnup SIMFUEL Measured After 24 (●) and 77 Hours (Δ) Immersion at Corrosion Potential Tested in a Simulated Groundwater With Calcium and Silicate Addition at 22 °C [72 °F] .....	3-14
3-11 Concentrations of Dissolved Metallic Species in Samples from SIMFUEL Corrosion Test After 3.25 Days at 22 °C [72 °F] .....	3-17
3-12 Converted Dissolution Rates of Uranium, Barium, Molybdenum, Strontium, and Zirconium After 3.25 Days of SIMFUEL Corrosion Test at 22 °C [72 °F].....	3-18
3-13 Changes in Aqueous Concentrations of Uranium, Barium, Chromium, Iron, Molybdenum, Nickel, Strontium, and Zirconium After Immersion of Stainless Steel Disk in Test Solutions for 21 Days .....	3-19
3-14 Potential-pH Diagrams for Uranium-Simulated Groundwater Systems at 22 °C [72 °F] at the Concentration of Dissolved Uranium Species of 10 <sup>-8</sup> M.....	3-20
3-15 Potential-pH Diagrams for Uranium-Simulated Groundwater Systems at 22 °C [72 °F] at the Concentration of Dissolved Uranium Species of 10 <sup>-7</sup> M.....	3-21
3-16 Potential-pH Diagrams for Uranium-Simulated Groundwater Systems at 22 °C [72 °F] at the Concentration of Dissolved Uranium Species of 10 <sup>-6</sup> M.....	3-21

## TABLES

Table	Page
1-1    Dissolution Rates in the Literature Relevant to the Test Conditions in Present Study.....	1-3
2-1    Chemical Composition of Stainless Steel Type 316L (in Weight Percent).....	2-2
2-2    Chemical Compositions of Test Solution {mg/L [mM]} .....	2-2
3-1    Chemical Compositions of SIMFUEL (in Weight Percent) .....	3-7
3-2    Calculated Dissolution Rates of SIMFUEL Obtained From Impedance Measurements.....	3-16

## ACKNOWLEDGMENTS

This report describes work performed by the Center for Nuclear Waste Regulatory Analyses (CNWRA®) and its contractors for the U.S. Nuclear Regulatory Commission (USNRC) under Contract No. NRC-02-07-006. The activities reported here were performed on behalf of the USNRC Office of Nuclear Material Safety and Safeguards, Division of High-Level Waste Repository Safety and Safeguards, Division of High-Level Waste Repository Safety. The USNRC staff views expressed herein are preliminary and do not constitute a final judgment or determination of the matters addressed or of the acceptability of any licensing action that may be under consideration at USNRC.

The authors gratefully acknowledge E. Percy for his technical review, J. Winterle for his programmatic review, L. Mulverhill for her editorial review, and A. Ramos for his administrative support. Special thanks to Mr. B. Derby for his assistance in conducting experiments in this study.

## QUALITY OF DATA, ANALYSES, AND CODE DEVELOPMENT

**DATA:** All CNWRA-generated original data contained in this report meet the quality assurance requirements described in the Geosciences and Engineering Division Quality Assurance Manual. Sources for other data should be consulted for determining the level of quality for those data. All data and calculations related to this report have been recorded in CNWRA Scientific Notebook 1022 (Jung, et al., 2011).

**ANALYSES AND CODES:** The Act2 component of Geochemist's Workbench Standard 6.0 (RockWare, Inc., 2005) was used in the analyses contained in this report. This software is commercial software controlled under the CNWRA quality assurance procedure Technical Operating Procedure-18. Documentation for the thermodynamic calculation in Section 2.2 can be found in Scientific Notebook 1022 (Jung, et al., 2011).

## References

Jung, H., B. Derby, and R. Pabalan. "Electrochemical Measurement of Spent Nuclear Fuel (SNF) Dissolution Rate Using Simulated Spent Fuel (SIMFUEL)." Scientific Notebook No. 1022. San Antonio, Texas: CNWRA. pp. 1-91. 2011.

RockWare, Inc. "Geochemist's Workbench Standard Version 6.0." Golden, Colorado: RockWare, Inc. 2005.

# 1 INTRODUCTION

This report is part of the knowledge management activities for the U.S. Nuclear Regulatory Commission high-level waste repository safety program. The report provides previously undocumented results from recent corrosion tests that used electrochemical methods, solution analyses, and thermodynamic computations to evaluate the corrosion behavior of simulated spent nuclear fuel (SIMFUEL) in a simulated groundwater at room temperature {e.g., 22 °C [72 °F]}. The corrosion experiments were conducted in aerated carbonate-based solutions with and without calcium and silicate addition. The dissolution rates of SIMFUEL were estimated by measuring polarization resistance and compared to corresponding rates obtained from solution analyses performed after corrosion tests. A potential effect of radionuclide sorption onto the oxides formed on stainless steel was also assessed.

## 1.1 Background Information

In a geologic disposal setting, spent nuclear fuel (SNF) degradation is considered an important process in assessing the potential for radionuclide releases. The degradation of SNF by contacting groundwater is expected to occur after containment components fail in a repository environment. The containment components usually include the canister, overpack (container), and/or cladding. Radionuclide release from SNF dissolution will determine the source term from the engineered barrier system (EBS) in assessing radionuclide transport from the disposal setting to the geosphere and further to the biosphere human environment. The EBS often includes the waste form, containment components, and backfill materials, if any. In assessing radionuclide release, long-lived (i.e., long half-life; thousands or more years) radionuclides are important because containment times are required to be long.

### Importance of SNF Dissolution Rates in Radionuclide Release

The SNF dissolution rate in groundwater is generally represented by the rate of uranium mass loss per unit area of the uranium dioxide (UO<sub>2</sub>) matrix. In assessing radionuclide release from SNF dissolution, two different types of radionuclides are considered (Wilson and Gray, 1990). The first type includes radionuclides such as Tc-99, I-129, C-14, and Cs-135. This type has high solubility limits and is expected to be released from SNF congruently with the SNF matrix dissolution rate. The congruent release rate is the same release rate of each radionuclide with respect to the total inventory of the radionuclide in the SNF matrix. The second type includes radionuclides such as Np-239, Pu-239, -240, -242, and U isotopes. This type has low solubility limits and tends to form precipitates on the surface of the SNF matrix, depending on the groundwater flow rate. In this case, the radionuclides are expected to be primarily released at the solubility limit of the radionuclides in the groundwater. Depending on the relative magnitude of the SNF dissolution rate, the groundwater flow rate, and the precipitation and the subsequent redissolution of precipitates, radionuclide release from SNF could be also be below the solubility limit. Therefore, for either of the two radionuclide types, it is important to determine the SNF dissolution rate in assessing radionuclide release from the EBS.

The SNF dissolution rate primarily depends on groundwater aqueous chemistry, conditions of SNF before groundwater contact, and groundwater contact modes (Ahn and Mohanty, 2008; Ferry, et al., 2005; Grambow, et al., 2000). Practically, the groundwater can be modified in the partially failed containment component by reaction with SNF or other internals in the containment component. The important groundwater chemical characteristics for SNF dissolution include carbonates, solution pH, cations dissolved in groundwater (e.g., calcium ions) and silicate, dissolved oxygen, oxidants (e.g., radiolysis products), and reducing species

(e.g., iron). Solution temperature is also important for the dissolution rate of SNF. The SNF dissolution rate usually increases with increases in carbonate concentration, temperature, and concentration of oxygen and oxidants, and decreases with an increase in reducing species toward neutral pH from acidic and alkaline sides. The conditions of SNF before groundwater contact include preoxidation/hydration of the SNF matrix and/or grain boundary opening of the SNF matrix during the reactor irradiation. These processes generally increase the SNF dissolution rate. The groundwater contact modes include aqueous immersion and groundwater dripping or flow. These modes could be specific to a disposal setting or to accelerated test methods. Therefore, the results from the tests with different modes usually need to be normalized with respect to the condition of the real, specific disposal setting.

The initial base data on SNF dissolution are typically obtained at room temperature in a solution of relatively simple water chemistry. As such, the work in this paper was done mainly in a carbonate solution with and without calcium and silicate. The carbonate concentration is limited to about 0.5 mM, and the concentrations of calcium and silicate are also limited to about 0.1 and 0.6 mM, respectively. This is typical of the solution concentrations expected after the containment period at Yucca Mountain or for similar disposal conditions. The pH condition is also limited to near neutral to slight alkaline range. Therefore, the background literature information is also very selective for this range of water chemistry. Table 1-1 presents selected data from the literature in a carbonate concentration range of about 0.1 to 10 mM; this is used as a basis to interpret the test results in this report. The literature information presented more data obtained under accelerated conditions such as higher carbonate concentration. The determination of effective surface area of the test sample is not trivial, because it involves factors such as the state of radionuclide distribution in the SNF matrix, grain boundary opening, surface roughening, and others as described in Ahn and Mohanty (2008). In Table 1-1, the samples Wilson and Gray (1990) used were pellets; others were powders with various sizes, ranging from 150  $\mu\text{m}$  to 0.5 mm [ $3.81 \times 10^{-2}$  to  $1.27 \times 10^{-1}$  in] with some of unknown size (by measuring the surface area by gas sorption). The dissolution rate per unit surface area is useful to scale test results from various test methods to real SNF. Various test methods require various sample sizes.

### SNF Dissolution Test Methods

The test methods are primarily designed to represent the SNF dissolution rate over a long period of time. The methods conducted to date can be divided into two broad categories—immersion tests and drip tests. Immersion tests have been conducted for the saturated disposal environment with groundwater, while drip tests have been conducted for the unsaturated dripping environment of groundwater. To understand mechanistically the results of immersion tests or drip tests, auxiliary flow-through or electrochemical methods are also used. High flow in these auxiliary tests can avoid possible blocking due to precipitate deposits on the reacting surface. As mentioned earlier, determining this unblocked dissolution rate is important in assessing radionuclide release. In the disposal environment, highly soluble radionuclides will not be deposited and the concentration of low soluble radionuclides will be determined by the unblocked dissolution rate, flow rate, and the rates of precipitate and its redissolution. Table 1-1 specifies the test method used for each datum. The method used in this study is electrochemistry.



Table 1-1. Dissolution Rates in the Literature Relevant to the Test Conditions in Present Study

Dissolution Rate, mg/m <sup>2</sup> -day	Sample Tested	Solution Chemistry	pH	Temperature	Test Methods	Notes	Reference*
0.63–2.5	UO <sub>2</sub>	1–10 mM [HCO <sub>3</sub> <sup>-</sup> ]	7.5–8.5	25 °C {[77 °F]}	Flow Through	—	Pablo, et al., 1999
About 9 (significant increase at low pH)	SNF	10 mM NaCl with 10 mM [HCO <sub>3</sub> <sup>-</sup> ]	pH>6 pH<6	Room Temperature	Flow Through	Congruent Dissolution of Np, Ba, Tc, Cs, Sr, Rb; Incongruent Dissolution: Zr, Mo, Ru, Rh, Pd, Am	Röllin, et al., 2001
6.0–9.1	CANDU UO <sub>2</sub>	0.5–1.0 mM [HCO <sub>3</sub> <sup>-</sup> ]		Room Temperature	Flow Through	—	Tait and Luht, 1997
0.4–3.9	SNF	Simulated Groundwater	8.4	25 °C [77 °F]	Immersion	Acid stripping and fission product release, Ca, 0.13 mM; Si, 0.61 mM; [HCO <sub>3</sub> <sup>-</sup> ], 0.61 mM	Wilson and Gray, 1990; Bechtel SAIC Company, 2004
2–9	UO <sub>2</sub> , SNF	0.2–20 mM [HCO <sub>3</sub> <sup>-</sup> ]	8–10	25 °C [77 °F]	Flow Through	—	Bechtel SAIC Company, 2004

## \*References

Pablo, J., I. Casas, J. Gimenez, M. Molera, M. Rovira, L. Duro, and J. Bruno. "The Oxidative Dissolution Mechanism of Uranium Dioxide I. The Effect of Temperature in Hydrogen Carbonate Medium." *Geochimica et Cosmochimica Acta*. Vol. 63. pp. 3,097–3,103. 1999.

Röllin, S., K. Spahiu, and U.-B. Eklund. "Determination of Dissolution Rate of Spent Fuel in Carbonate Solutions Under Different Redox Conditions With a Flow-Through Experiment." *Journal of Nuclear Materials*. Vol. 297. pp. 231–243. 2001.

Tait, J.C. and J.L. Luht. "Dissolution Rates of Uranium from Unirradiated UO<sub>2</sub> and Uranium and Radionuclides from Used CANDU Fuel Using the Single-Pass Flow-Through Apparatus." 06819–REP–01200–0006 R00. Canada: Atomic Energy of Canada Ltd., Whiteshell Laboratories. 1997.

Wilson, C.N. and W.J. Gray. "Measurement of Soluble Nuclide Dissolution Rates From Spent Fuel." Symposium Proceedings. Warrendale, Pennsylvania: Materials Research Society. Vol. 176. pp. 489–498. 1990.

Bechtel SAIC Company, LLC. "CSNF Waste Form Degradation: Summary Abstraction." Rev. 2. ANL–EBS–MD–000015. Las Vegas, Nevada: Bechtel SAIC Company, LLC. 2004.

Note: Surface area measurements are normalized with the geometric surface area, assuming a factor of three increase in the BET surface area compared to the geometric surface area (Bechtel SAIC Company, 2004).

## New Waste Forms

Currently, the United States has commercial SNF, U.S. Department of Energy-owned SNF, Navy SNF, and defense high-level waste (HLW) glass. In the future, new waste forms may need to be managed. Commercial SNF may have higher burnup, and spent mixed-oxide fuel (sMOX) with various burnups may be present. Defense HLW glass may have higher waste loading. If the nation pursues various types of reprocessing and/or transmutation of commercial SNF, other types of waste forms may be present. These may include new HLW glass, HLW ceramics (or glass ceramics), and metallic waste forms, varying waste loading. Additionally, the new waste forms may have very selective radionuclide loading, depending on the types of reprocessing and/or transmutation, if available. In this case, ceramics or metallic waste forms with single or fewer types of radionuclides may be expected. For example, I-129 or Pu-239 encapsulated ceramics or metallic waste forms may be present.

Metallic waste forms are primarily expected from pyro-reprocessing. Metallic waste forms are specifically addressed in this report because the test methods of their aqueous performance may include electrochemical methods as an effective tool to estimate dissolution rates of the metallic waste form. sMOX tests are also likely to use electrochemistry. Metallic waste form tests currently use immersion, flow-through, or electrochemical methods.

Argonne National Laboratory (ANL) has developed an electrometallurgical treatment for SNF from the experimental breeder reactors II. A product of this treatment process is a metal waste form that incorporates the stainless steel cladding hulls, zirconium from the SNF, and fission products that are noble to the process (i.e., technetium, rubidium, niobium, palladium, rodium, and silver). The metal waste form was crushed and tested for dissolution under immersion conditions (Johnson, et al., 2000). ANL also conducted dissolution tests of a similar metallic waste form, and the results were compared with glass dissolution rates, using highly soluble boron release as the indicator of the dissolution in pH-buffered solutions at 50, 70, and 90 °C [122, 158, and 194 °F] (Ebert, et al., 2003). Figure 1-1 shows the results. More recently, metallic waste form tests were considered to be standardized by electrochemical methods (Cunnane, et al., 2010).

## Sorption

In determining the source term of radionuclide release from the EBS, it is also important to assess radionuclide sorption on the surface of corrosion products of container or canister metals. Retardation of radionuclides by sorption is more pronounced for low-solubility radionuclides such as Pu and U. The sorption capacity also depends on the radionuclide concentration in the groundwater. Therefore, the sorption capacity will vary near to or far from the waste form. In this study, stainless steel coupons (forming iron oxides on the surface) are also immersed in the electrochemical test cell to assess radionuclide sorption capacity near SIMFUEL during its dissolution as discussed in Chapter 2.

## Simulated Spent Nuclear Fuel

SIMFUEL is an un-irradiated analog of irradiated SNF, produced by doping natural uranium dioxide (UO<sub>2</sub>) matrix with a series of nonradioactive elements in appropriate proportions that can replicate the chemical and microstructural effects of irradiation on UO<sub>2</sub> fuel at various degrees of burnups in a reactor (Lucuta, et al., 1991). Nonradioactive elements (e.g., barium, cerium, lanthanum, molybdenum, strontium, yttrium, zirconium, rhodium, palladium, ruthenium, and

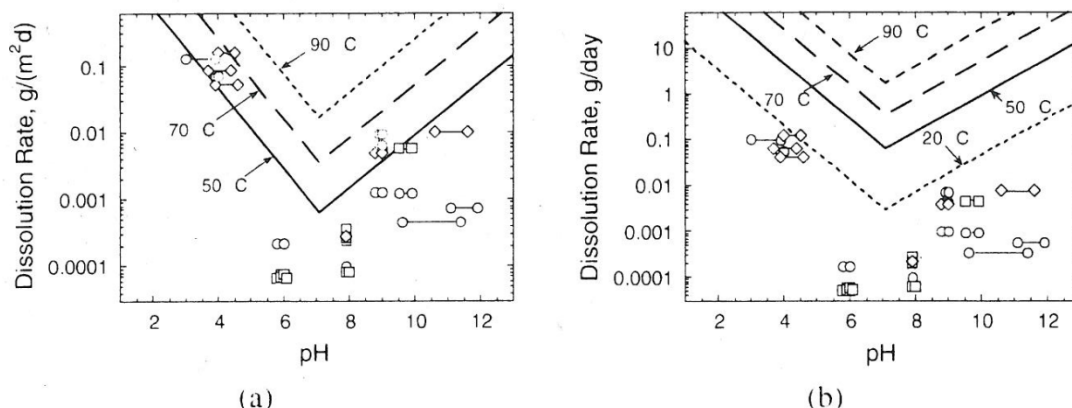


**Figure 1-1. Comparison of Dissolution Rate of Metallic Waste Form at (a) 50 °C (□) 70 °C (◇) 90 °C [122, 158, and 194 °F] With Rates From HLW Glass Model: (a) Specific Dissolution Rate and (b) Dissolution Rate. Lines Connecting the Symbols Show the Range of pHs Attained in Each Test.**

neodymium) in SIMFUEL can represent most fission products present in an irradiated SNF, including oxide dissolved in the matrix, metallic precipitates, and oxide precipitates (except volatile fission gases). A general trend was observed where higher burnup of  $\text{UO}_2$  fuel in a water-reactor can result in more fission products for SNF and sMOX. Thus, SIMFUEL can provide a convenient way to study different burnup effects on fuel properties such as thermal conductivity and diffusivity (Lucuta, et al., 1995), and degradation behavior (e.g., oxidation and dissolution) (Choi, et al., 1996; Rondinella and Mazke, 1996; Bruno, et al., 1992; Santos, et al., 2006a) without complication of an intense radiation field. The use of irradiated SNF for dissolution experiments poses significant constraints (e.g., use of hot cell) on the experimental conditions and the characterization techniques that can be used.

In addition, the use of SIMFUEL can avoid accelerated radiolysis effects, in particular on dissolution of SNF due to the relatively strong gamma/beta radiation field from SNF during an initial repository period after closure. The waste package failures could occur much later, when a level of gamma/beta radiation is expected to be several orders of magnitude lower and ineffective or negligible on radiolysis of water. Therefore, results from dissolution experiments using irradiated (young aged) SNF samples could not be directly applied to the repository-relevant conditions.

Fission products in a real SNF can be typically classified into four groups (Lucuta, et al., 1991).

- Oxides dissolved in the matrix: strontium, zirconium, niobium, yttrium, lanthanum, cerium, praseodymium, neodymium, promethium, samarium
- Metallic precipitates {mostly  $\epsilon$ -phase, 0.5–1.5  $\mu\text{m}$  in diameter
- $[1.27 \times 10^{-4} - 3.81 \times 10^{-4} \text{ in}]$ : molybdenum, technetium, ruthenium, rhodium, palladium, silver, cadmium, indium, antimony, tellurium

- Oxide precipitates {perovskite phase, fine particle about 0.1  $\mu\text{m}$  diameter [ $2.54 \times 10^{-5}$  in]: barium, zirconium, niobium, molybdenum (rubidium, cesium, tellurium)
- Gases and other volatile elements: krypton, xenon, bromine, iodine (rubidium, cesium, tellurium)

### Usefulness of Electrochemical Method in Applying Corrosion of SNF

Electrochemical methods have been extensively used to develop both understanding of the dissolution process and the framework of a model that can predict SNF dissolution rates as a function of evolving redox and environmental conditions using un-irradiated  $\text{UO}_2$  or SIMFUEL pellets. Canadian and European research groups use these methods because dissolution of  $\text{UO}_2$  under oxidizing conditions is an electrochemical corrosion reaction (Shoesmith and Sunder, 1998). Shoesmith, et al. (1996) attempted to validate an electrochemical model for oxidative dissolution of used CANDU fuel by comparing the predicted dissolution rates based on a model to the measured rates for  $\text{UO}_2$  and SNF powder measured in flow-through experiments on  $\text{UO}_2$  and used CANDU fuels. Comparison of the results demonstrated that the predicted and measured rates are close, in particular for the case of the aerated carbonate solutions in relatively oxidized potentials (e.g.,  $\geq -100 \text{ mV}_{\text{SCE}}$ ), and the dependence of the rates on carbonate is almost the same—in a range of 0.1 mM to 0.4 M  $\text{HCO}_3^-$ . That good agreement confirms that  $\text{UO}_2$  dissolution can be predicted by appropriate electrochemical measurements in the case of particularly oxidizing conditions with carbonate-containing solutions [carbonate has a strong complexing ability for U(IV)]. In neutral, noncomplexing solutions (e.g., pure chloride solution without carbonate), however, models do not properly predict the dissolution rate when secondary phases such as schoepite form on the fuel surface.

One electrochemical method that can be effectively applied for evaluating dissolution behavior of  $\text{UO}_2$  or SNF is electrochemical impedance spectroscopy (EIS). This technique has been extensively used for study in the areas of corrosion, semiconductors, batteries, concrete degradation and rebar corrosion, coating degradation, and electroplating. By applying a very small external AC voltage or current perturbation to drive the electrode-environment interface not far from the steady state, a wealth of kinetic (i.e., dissolution rate) and mechanistic information at the fuel and solution interface can be obtained in real time. In particular, this technique can be a very effective tool in conducting corrosion experiments on high resistivity electrodes such as  $\text{UO}_2$  and SNF and also in a very low conductivity solution where DC polarization methods are subject to significant potential drop. EIS can also be applied to such a neutral, noncomplexing solution in which secondary phases can form to estimate more accurately the dissolution rate of  $\text{UO}_2$ , which was difficult to measure using conventional leaching tests or conventional electrochemical methods (e.g., cyclic voltammetry, potentiodynamic or galvanostatic polarization). Impedance responses from EIS measurement can separate a net corrosion resistance of a  $\text{UO}_2$  matrix from a resistance from a secondary phase by using an appropriate electrical circuit model to fit. To date, European researchers reported a few studies on  $\text{UO}_2$  dissolution behavior using EIS (Bottomley, et al., 1996; Engelhardt, et al., 1996; Miserque, et al., 2001).

## **1.2 Objective and Scope**

The objectives of the present work are (i) to confirm the range of dissolution rates of SNF in a repository relevant environment, specifically under an oxidizing condition, by using SIMFUEL as an analog material and (ii) assess a potential effect of radionuclide sorption onto the oxides formed on stainless steel. In addition, the thermodynamic stability of uranium in a simulated

water is examined by utilizing the potential-pH diagrams for uranium-simulated groundwater systems at a relatively low temperature such as 22 °C [72 °F].

SIMFUEL and electrochemical methods used to evaluate dissolution of SNF were described in this chapter. The importance of dissolution rates of SNF in radionuclide release with a list of relevant literature data on dissolution rate measurement were also discussed in this chapter.

Experimental conditions in this study are provided in Chapter 2, including details of test samples, test solutions, and test procedures. Results of experiments and analyses are discussed in Chapter 3 including characterization results of SIMFUEL, electrochemical measurements (i.e., corrosion potential and impedance), solution chemistry analyses after corrosion testing, and sorption test results. A thermodynamic stability assessment for uranium-simulated groundwater system is also discussed in Chapter 3. Chapter 4 provides the study conclusions.

## 2 EXPERIMENTAL DETAILS

### 2.1 Materials

The working electrodes used for the corrosion tests were disk-shaped SIMFUEL pellets simulating SNF with a 3 or 6 atomic percent burnup level. As described in the previous section, these SIMFUEL pellets are natural  $\text{UO}_2$  pellets doped with nonradioactive elements. The SIMFUEL samples were provided by European Commission (EC)-Institute for Transuranium Element (ITU) in Germany and originally fabricated at Atomic Energy of Canada Limited (AECL). The SIMFUEL pellets were 2 to 3 mm [0.08 to 0.12 in] thick and 12 mm [0.47 in] in diameter. To enable rotation of the SIMFUEL working electrode, the SIMFUEL disk was inserted into a threaded Teflon<sup>®</sup> cylinder and the inner face of the disk was bonded to a stainless steel wire with a highly conductive silver epoxy. After curing the epoxy for 24 hours, the Teflon cylinder containing the SIMFUEL disk was attached to the rotator (Pine Instruments Model) and lowered into the test solution for use in the experiment. Prior to use, the SIMFUEL electrode was polished to a 1,200-grit finish, cleaned with ethanol, and dried. Lucuta, et al. (1991) discussed in detail the preparation and microstructural features of this type of SIMFUEL. The microstructures and chemical compositions of the SIMFUEL samples used for this study were analyzed, and the results are discussed in Section 3.1.

For the sorption test, a stainless steel Type 316L disk was used. The disk was 6.35 mm [0.25 in] thick and 20.32 mm [0.8 in] in diameter. The stainless steel disk was polished to a 1,200-grit finish, cleaned with ethanol, and dried before immersion in the solution. The chemical composition of stainless steel Type 316L is shown in Table 2-1.

### 2.2 Test Solutions

Two different concentrations of carbonate-based solutions (i.e., simulated groundwater and in-package chemistry water) were used. The chemical compositions of the test solutions, which are shown in Table 2-2, were selected based on literature data (Wilson and Gray, 1990; Finn, et al., 1998; Sandia National Laboratory, 2007). The solutions were prepared from reagent-grade chemicals. The initial solution pHs were adjusted to 8 and 7 for a simulated groundwater and an in-package chemistry water, respectively. The solution pH was monitored with an Orion glass electrode and an Orion model 290A pH meter. The test solution was aerated by keeping the test vessel open to air.

### 2.3 Test Procedures

The electrochemical tests were conducted at room temperature  $\{22 \pm 2 \text{ }^\circ\text{C} [72 \pm 3.6 \text{ }^\circ\text{F}]\}$  in a 200-mL [0.05-gal] glass cell. A saturated calomel reference electrode was interfaced to the test solution via a salt bridge filled with the test solution. A platinum foil was used as a counter electrode. The experimental setup is presented in Figure 2-1.

The average exposed surface area of the SIMFUEL working electrodes was  $1.13 \text{ cm}^2$  [0.175 in<sup>2</sup>]. In the tests using simulated groundwater, the test samples were rotated at a speed of 1,000 rpm, whereas in the tests using in-package chemistry water, the tests samples were not rotated (quiescent). Impedance measurements were carried out in the frequency range of 100 kHz to 0.1 mHz with an alternating current voltage amplitude of 20 mV at the corrosion potential. All electrochemical experiments were performed with a potentiostat (VMP3 model)

Table 2-1. Chemical Composition of Stainless Steel Type 316L (in Weight Percent)										
Fe	Cr	Ni	Mo	Mn	Si	Cu	N	P	S	C
Balance	16.43	10.13	2.06	1.35	0.51	0.32	0.022	0.027	0.0006	0.019

Fe = iron, Cr = chromium, Ni = nickel, Mo = molybdenum, Mn = manganese, Si = silicon, Cu = copper, N = nitrogen, P = phosphorous, S = sulfur, C = carbon

Table 2-2. Chemical Compositions of Test Solutions {mg/L [mM]}		
Chemicals	Simulated Groundwater (pH = 8)	In-Package Chemistry Water (pH = 7)
NaCl	14.0 [0.24]	11.2 [0.2]
NaHCO <sub>3</sub>	51.2 [0.61]	16.8 [0.2]
Na <sub>2</sub> SiO <sub>4</sub> •5H <sub>2</sub> O	13.9 [0.61]	22.8 [0.1]
CaCl <sub>2</sub>	14.4 [0.13]	5.6 [0.05]

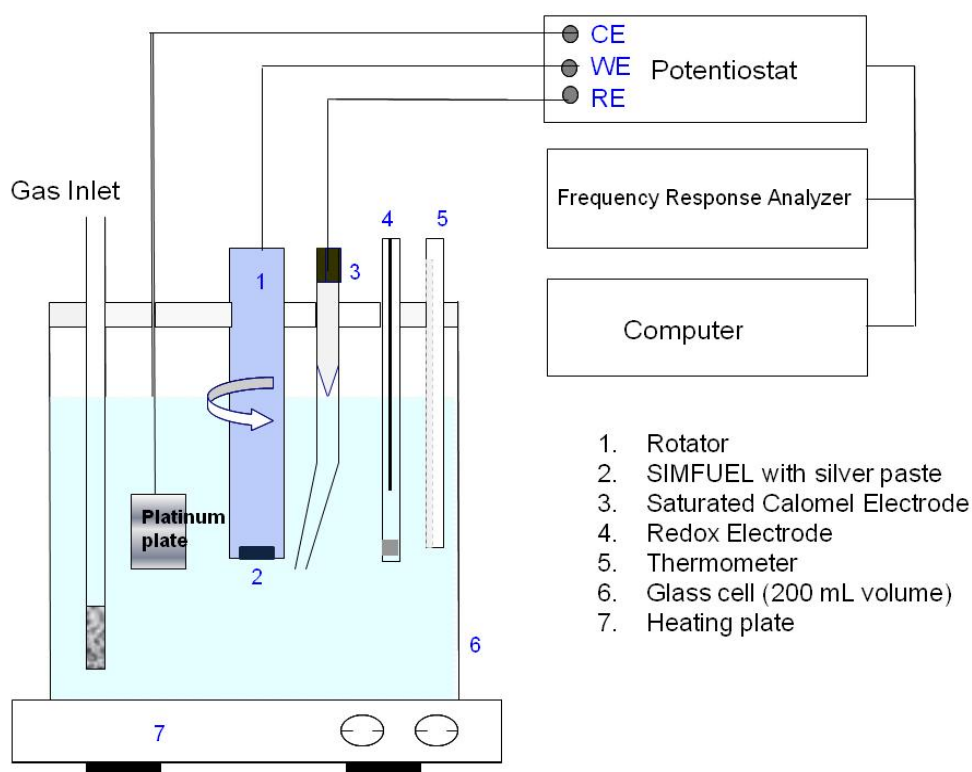


Figure 2-1. Experimental Setup for Electrochemical Test

controlled by EC-Lab software. The measured potentials are referenced to a saturated calomel reference electrode (SCE) via the conversion given in (Eq. 2-1).

$$E(V_{SCE}) = E(V_{SHE}) - 0.242\text{ V} \quad (2-1)$$

After completion of the tests, 40-mL [1.353-fl oz] samples of each test solution were taken, acidified by adding 250  $\mu\text{L}$  [ $8.45 \times 10^{-3}$  fl oz] of concentrated nitric acid, and saved for later chemical analysis.

A sorption test subsequently was conducted by transferring 40 mL [1.353 fl oz] of the posttest solutions into glass cells and immersing a stainless steel disk in each solution. The experimental setup for the sorption test is presented in Figure 2-2. The solutions during the test were mildly stirred using a small magnetic stirrer. After 21 days, the disks were taken out and the solutions were acidified and saved for later chemical analysis.

The chemistry of the solution samples and two blank solutions (i.e., simulated groundwater with and without Ca and Si) were analyzed using inductively coupled atomic emission spectrometry (ICP-AES) or inductively coupled plasma mass spectrometry (ICP-MS). ICP-AES was used to determine calcium and silicon concentrations, and ICP-MS was used to measure barium, chromium, iron, molybdenum, nickel, strontium, uranium, and zirconium concentrations.



**Figure 2-2. Experimental Setup for Sorption Test**



### 3 RESULTS AND DISCUSSION

This section summarizes and discusses the results of experiments and analyses including SIMFUEL characterization, electrochemical testing, non-electrochemical solution chemistry analysis after corrosion testing, and sorption testing. Finally, thermodynamic stability calculation results for uranium and simulated water systems are discussed.

#### 3.1 SIMFUEL Characterization

##### 3.1.1 Microstructure

To establish similitude of microstructure and composition of SIMFUEL with specimens of actual SNF, microscopy images were compared with those produced in previous work. In addition, to evaluate consistency with other SIMFUEL production batches, the metallographic results were compared with published results from earlier work on SIMFUEL. The microstructure of SIMFUEL samples was characterized using optical and scanning electron microscopy. Because the as-polished SIMFUEL samples did not clearly show grain boundaries on any precipitates, if present, the SIMFUEL samples were chemically etched by immersion for 3 minutes in an etchant composed of sulfuric acid (1 volume percent), hydrogen peroxide (2 volume percent), and distilled water (7 volume percent) at room temperature following the procedures reported in the literature (Ishii and Seki, 1967).

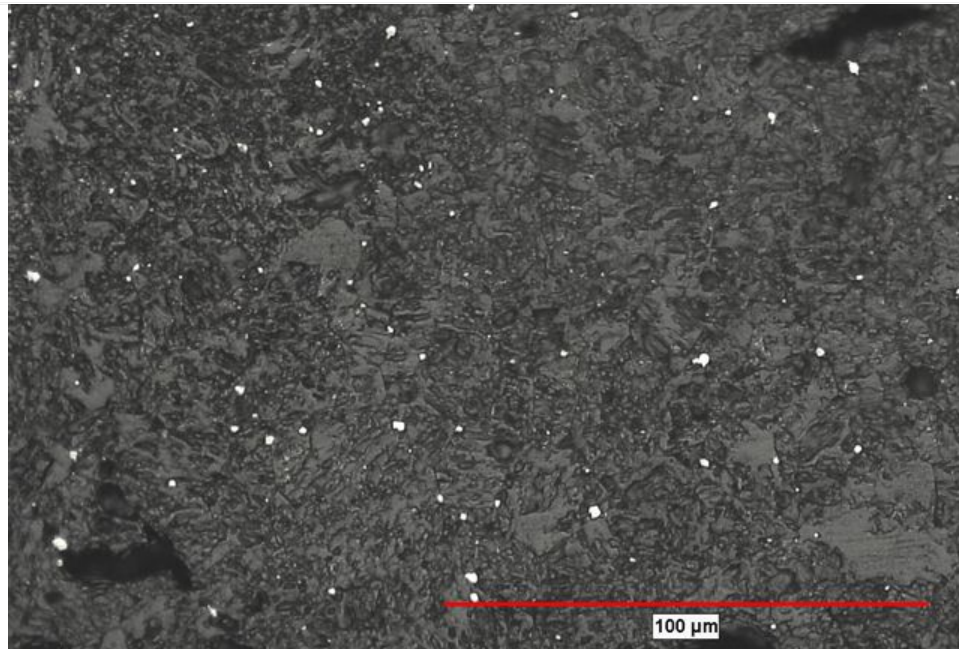
The optical micrograph of the surface of 3 and 6 percent burnup SIMFUEL specimens is shown in Figure 3-1(a,b), respectively. As seen in the figures, both SIMFUEL specimens reveal a compact surface without clear evidence of voids or cracks. Therefore, in estimating the dissolution rate of SIMFUEL samples, the geometric surface area of  $1.13 \text{ cm}^2$  [ $0.175 \text{ in}^2$ ] was used for analysis purposes in this study.

The surface also includes many small-sized precipitates (seen as the white particles in the figures) that are present mainly along grain boundaries. Grain sizes, determined by the linear interception method, were approximately  $15 \text{ }\mu\text{m}$  [ $5.91 \times 10^{-4} \text{ in}$ ] for the 3 percent burnup specimen and  $< 10 \text{ }\mu\text{m}$  [ $3.94 \times 10^{-4} \text{ in}$ ] for the 6 percent burnup specimen. Lucuta, et al. (1991) reported a similar microstructure on the 6 percent burnup SIMFUEL, showing spherical, intergranular metallic precipitates { $0.5\text{--}1.5 \text{ }\mu\text{m}$  [ $1.97 \times 10^{-5}\text{--}5.91 \times 10^{-5} \text{ in}$ ] diameter} along the grain boundary. In the same reference, the analysis results of the metallic precipitates indicated that the precipitates consisted of mainly  $\epsilon$ -phase (hexagonal close packed, hcp) and average composition yielded 28 atomic percent Mo, 47 atomic percent Ru, 3 atomic percent Rh, and 22 atomic percent Pd. In the same reference, the grain size of 6 percent burnup was estimated to average  $12 \text{ }\mu\text{m}$  [ $4.72 \times 10^{-4} \text{ in}$ ].

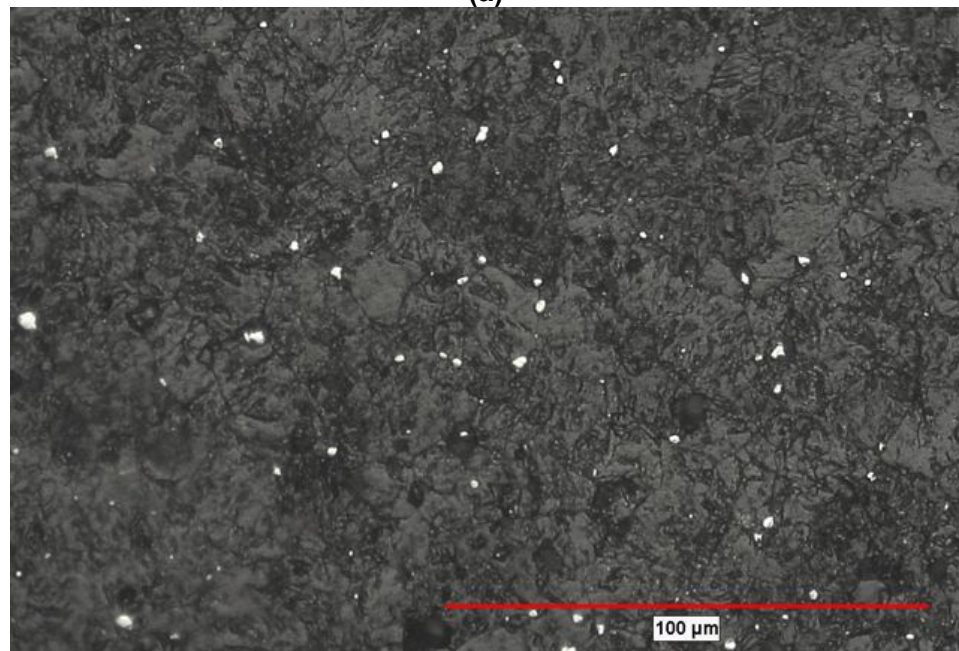
The microstructures of SIMFUEL samples in this study were correlated with those produced by prior research on SIMFUEL (Lucuta, et al., 1991; Park, et al., 2008), irradiated  $\text{UO}_2$  (Ishii and Seki, 1967), and SNF (Rondinella and Wiss, 2010).

##### 3.1.2 Chemical Composition

The chemical composition of both the 3 and 6 percent burnup SIMFUEL specimens was determined by energy dispersive X-ray (EDX) analysis. The areas examined are shown in Figure 3-2(a,b) for 3 and 6 percent burnups, respectively.



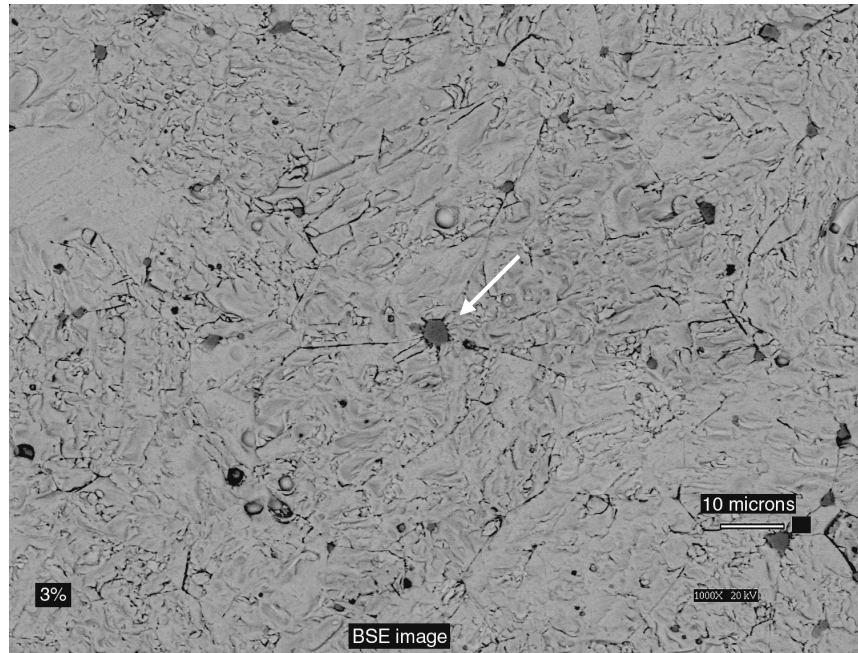
(a)



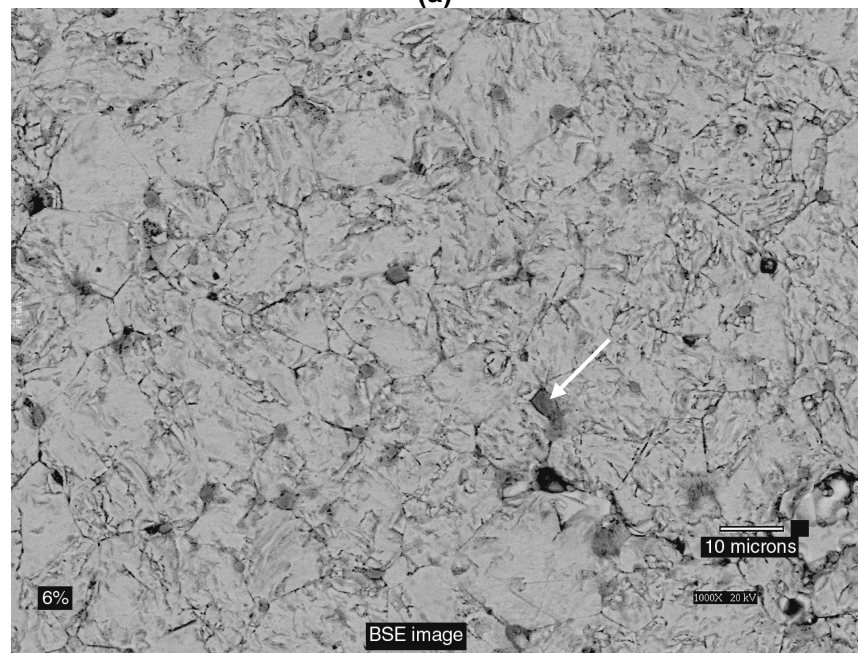
(b)

**Figure 3-1. Optical Micrographs of SIMFUEL Surfaces: (a) 3 Percent Burnup and (b) 6 Percent Burnup**

---



(a)



(b)

**Figure 3-2. Backscattered Electron Micrographs of SIMFUEL Surfaces: (a) 3 Percent Burnup and (b) 6 Percent Burnup**

These backscattered images can more easily identify these precipitates as the darker area, indicating lighter atomic compositions of these precipitates compared to the near-matrix area. The majority of precipitates are present mainly along the grain boundary and triple junctions and rarely present inside the grain. The corresponding EDX spectra are shown in Figures 3-3 and 3-4 for 3 and 6 percent burnup, respectively.

Table 3-1 summarizes chemical analysis results for 3 and 6 percent burnup SIMFUEL in this study for the two different areas: general surface area {~200  $\mu\text{m}$  by 200  $\mu\text{m}$  [ $5.08 \times 10^{-2}$  by  $5.08 \times 10^{-2}$  in]} and grain boundary precipitate only. The arrows marked in Figure 3-2 indicate the local area of grain boundary precipitates for EDX analysis.

For the case of the general surfaces in both 3 and 6 percent burnups, SIMFUEL matrix consists of predominant  $\text{UO}_2$  and the contents of U are in good agreement with the data reported in the literature for the 3 and 6 percent burnup SIMFUEL pellets manufactured by AECL (Lucuta, et al., 1991; Rondinella and Matzke, 1996). In the literature, the contents of U were 97.449 and 94.866 wt% for 3 and 6 percent burnups, respectively, which are very close to the U contents (i.e., 97.46 and 95.02 wt% for 3 and 6 percent burnups, respectively) observed in this study. The other elements (except U) to represent fission products accordingly increase with burnup (i.e., 2.54 and 4.98 wt% for 3 and 6 percent burnups, respectively). Compared to 3 percent burnup SIMFUEL, the surface of 6 percent burnup SIMFUEL appears to have more precipitates along the grain boundaries indicating a more heterogeneous nature. A higher content of elements other than U may result in more precipitates. The size of precipitates on 6 percent SIMFUEL is similar to the size on 3 percent SIMFUEL.

The precipitates consisted of predominantly molybdenum, ruthenium, palladium, and rhodium, which is in agreement with analysis results from earlier SIMFUEL production batches (Lucuta, et al., 1991). Also note that other transition metallic elements (i.e., Fe, Ni, and Cr) were detected in the precipitates; these were not the contents in the metallic precipitates reported in the works referenced previously. These transition metallic elements were confirmed from the solution chemistry analysis as discussed in Section 3.3.

In the general surface area, other elements such as strontium, zirconium, lanthanum, cerium, neodymium, and barium were detected. These were not detected at the grain boundary precipitates. Results of SIMFUEL analysis by Lucuta, et al. (1991) indicate that strontium, zirconium, and rare earth elements (cerium, lanthanum, neodymium) were fully or partially dissolved in the matrix grains. For the case of barium, Lucuta, et al. (1991) also observed that barium was a major element for the very small-sized oxide precipitates {about 0.1  $\mu\text{m}$  [ $3.94 \times 10^{-6}$  in]} present at grain boundary.

Attributes assessed in the comparisons were grain size, morphology, precipitates content, and elemental composition and distribution. The images obtained in the as-polished condition showed the precipitates' content was similar to that observed by prior researchers of SIMFUEL, irradiated  $\text{UO}_2$ , and SNF.

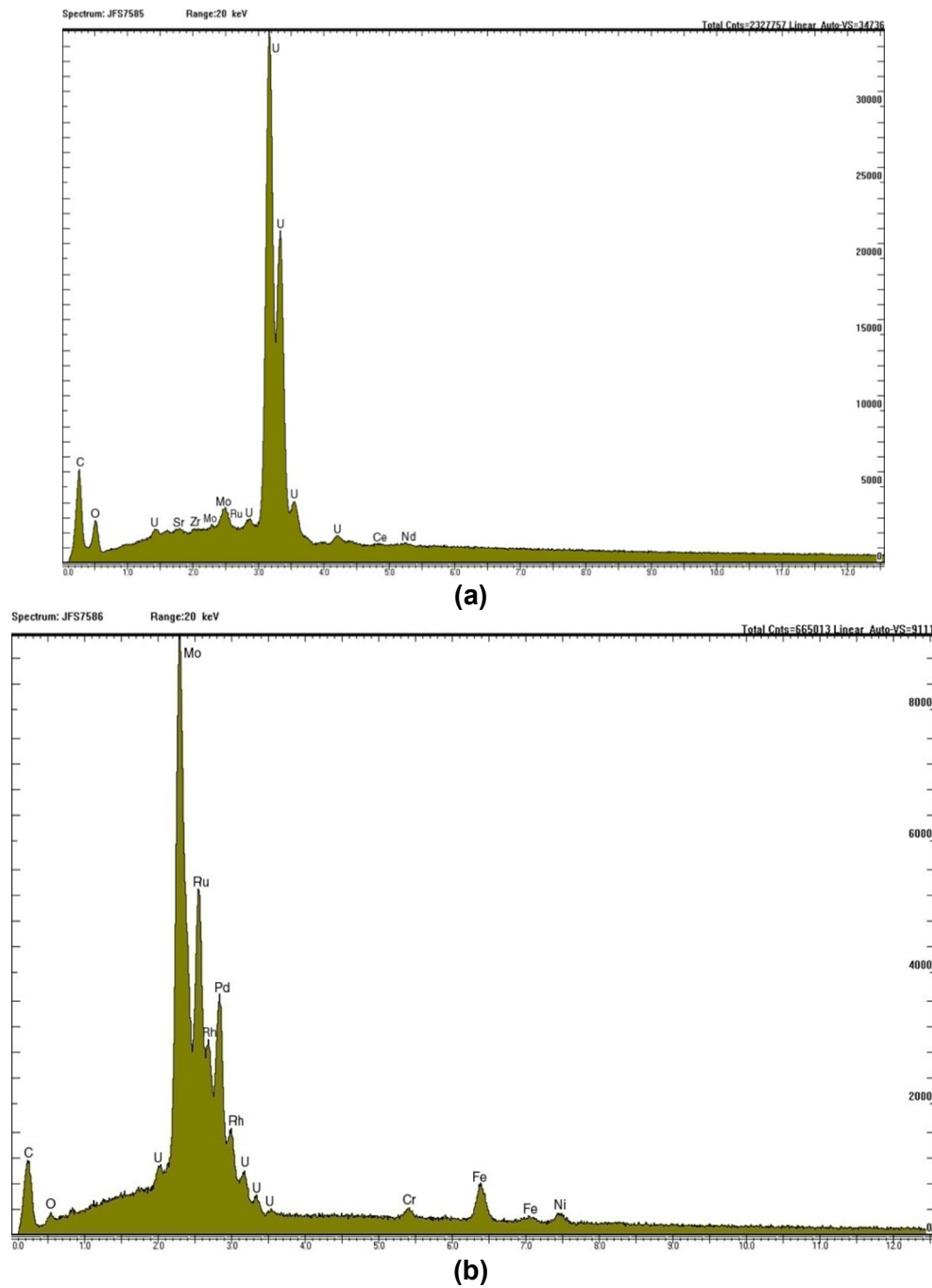


**Figure 3-3. Energy Dispersive Spectra of 3 Percent Burnup SIMFUEL: (a) Overall Surface and (b) Grain Boundary Precipitates**

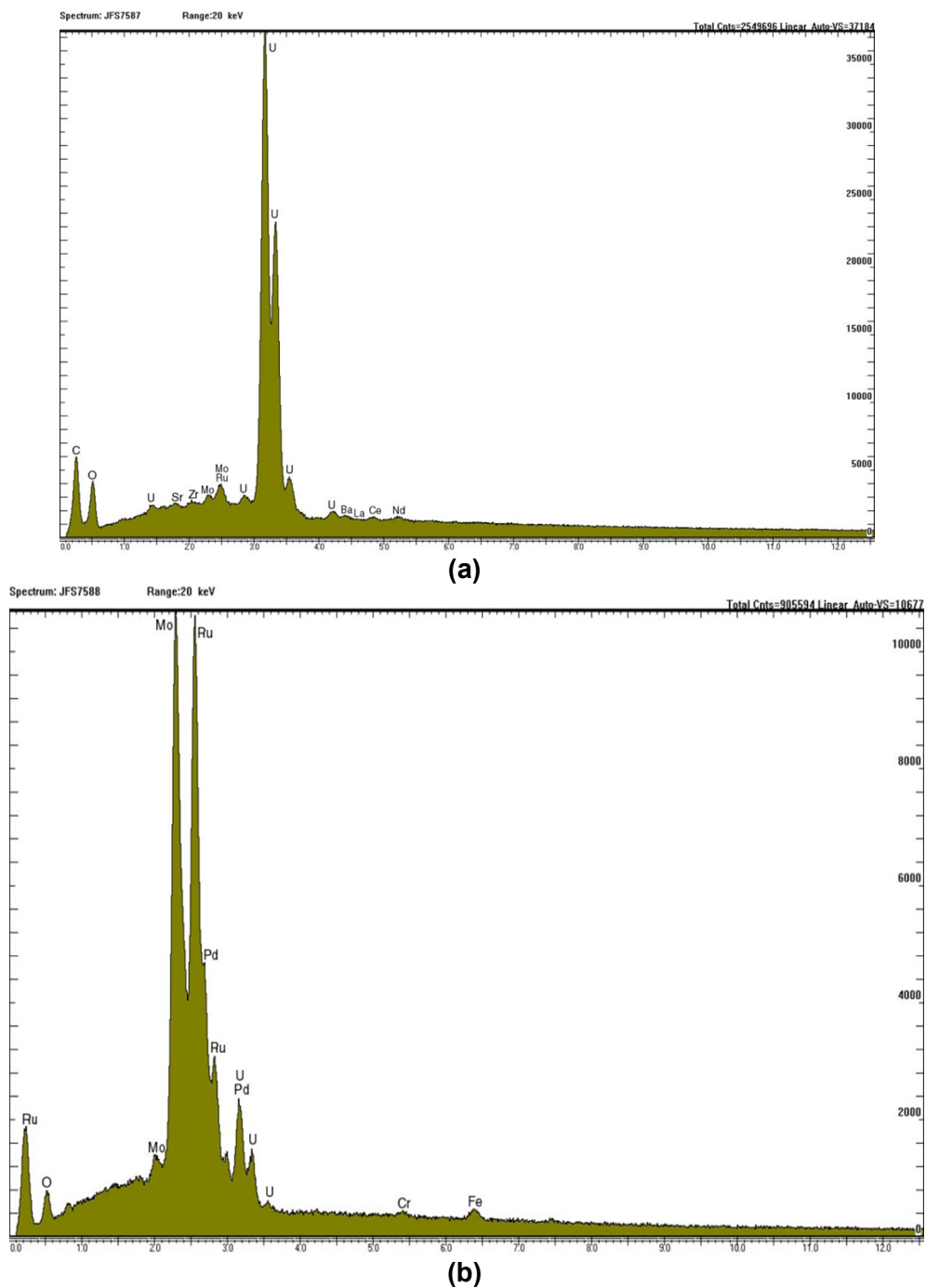


**Figure 3-4. Energy Dispersive Spectra of 6 Percent Burnup SIMFUEL: (a) Overall Surface and (b) Grain Boundary Precipitates**

<b>Table 3-1. Chemical Compositions of SIMFUEL Samples (in Weight Percent)</b>				
<b>Element</b>	<b>3 Percent Burnup</b>		<b>6 Percent Burnup</b>	
	<b>General Surface</b>	<b>Grain Boundary Precipitate</b>	<b>General Surface</b>	<b>Grain Boundary Precipitate</b>
U	97.46	6.21	95.02	16.38
Sr	0.37	<0.01	0.34	<0.01
Y	<0.01	<0.01	<0.01	<0.01
Zr	0.55	<0.01	0.73	<0.01
Mo	0.49	39.25	1.11	30.47
Ru	0.51	28.66	0.52	42.02
Rh	<0.01	3.72	<0.01	<0.01
Pd	<0.01	18.09	0.21	10.05
Ba	<0.01	<0.01	0.64	<0.01
La	<0.01	<0.01	0.28	<0.01
Ce	0.37	<0.01	0.66	<0.01
Nd	0.24	<0.01	0.49	<0.01
Cr	<0.01	0.63	<0.01	0.26
Fe	<0.01	3.42	<0.01	0.81
Ni	<0.01	1.31	<0.01	<0.01
U = uranium, Sr = strontium, Y = yttrium, Zr = zirconium, Mo = molybdenum, Ru = rubidium, Rh = rhodium, Pd = palladium, Ba = barium, La = lanthanum, Ce = cerium, Nd = neodymium, Fe = iron, Cr = chromium, Ni = nickel				

## 3.2 Electrochemical Testing

Two electrochemical techniques were employed: corrosion potential and impedance spectroscopy. The corrosion potential can provide information on a possibly stable oxidation state of uranium of the SIMFUEL surface by comparing it with the literature data on the well-established relationship between corrosion potential and the oxidation state of uranium (Shoesmith, et al., 1996). The measured corrosion potential can be also used in interpreting thermodynamic stability calculations of uranium and water systems as discussed in Section 3.2.4. The main purpose of impedance measurement was to estimate a real-time dissolution (corrosion) rate of SIMFUEL by utilizing both the Stern-Geary equation and Faraday's law.

### 3.2.1 Corrosion Potential Versus Time

Figure 3-5 shows the corrosion potential of a 3 percent burnup SIMFUEL electrode as a function of time in simulated groundwater without and with calcium and silicate addition (here after referred to as the "without case" and the "with case") at 22 °C [72 °F]. Corrosion potentials gradually increased with time and reached 0.122 and 0.082  $V_{SCE}$  for the without and with cases, respectively, after 72 hours. The corrosion potentials of SIMFUEL observed in this study are consistent with the reported values in the literature. In Shoesmith and Sunder (1998) and Shoesmith, et al. (1996), the measured corrosion potentials of SIMFUEL electrodes ranged from approximately 0.0 to 1.2  $V_{SCE}$  in aerated neutral or weakly alkaline solutions containing chloride and/or carbonate ions and were not different from those of un-irradiated  $UO_2$  or irradiated SNF. In this potential range, Shoesmith and Sunder (1998); Shoesmith, et al. (1996) suggested that the  $UO_2$  surface can be oxidized to produce  $UO_{2.333}$  film and further precipitate a secondary



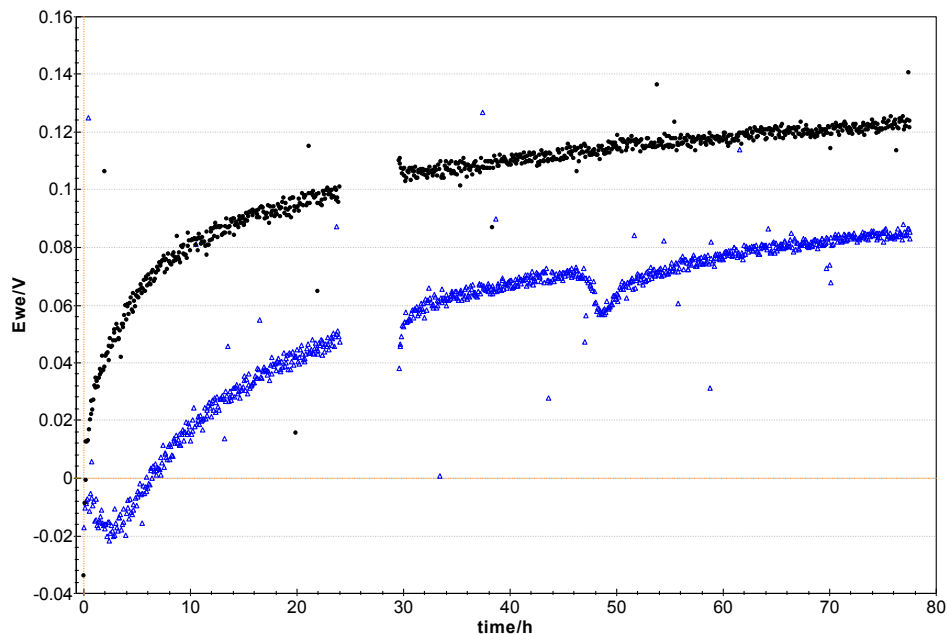


**Figure 3-5. Corrosion Potential Changes of 3 Percent Burnup SIMFUEL Electrode With Time Tested in a Simulated Groundwater Without (●) and With (Δ) Calcium and Silicate Addition at 22 °C [72 °F]**

phase (in the form of  $\text{UO}_3 \cdot x\text{H}_2\text{O}$ ) and/or dissolve to  $\text{UO}_2(\text{CO}_3)_2^{2-}$  depending on the solution chemistry. With the addition of calcium and silicate, as seen in Figure 3-5, the corrosion potential increased more slowly with time compared to the without case. This slow change and a relatively lower corrosion potential with the addition indicates a possible involvement of calcium and silicate in the reactions at the SIMFUEL surface. It has been reported that addition of calcium and silicate suppressed fuel dissolution rates when either single-pass flow-through tests (Wilson and Gray, 1990) or electrochemical tests (Santos, et al., 2006a,b) were conducted. Wilson and Gray (1990) reported that the addition of 15 mg/L of  $\text{Ca}^{2+}$  decreased the concentration of uranium in the effluent solution by a factor of 3 and further decreased by a factor of 100 with the addition of 30 mg/L of  $\text{SiO}_4^{4-}$ . More recently, Santos, et al. (2006a,b) also observed a similar suppression effect of calcium and silicate on the anodic dissolution of SIMFUEL. Santos, et al. (2006a) suggested that the suppression by  $\text{Ca}^{2+}$  in the solution was due to either inhibiting the stabilization of the cation precursor  $\{\text{UO}_2(\text{OH})_2\}_{\text{ads}}$  or blocking the

$\text{O}^{2-}$  anion transfer reaction from the fuel surface. In the case of silicate effect (Santos, et al., 2006b), a suppression was due to adsorption of silicate on the fuel surface and particularly at high anodic potentials (i.e.,  $>0.25 \text{ V}_{\text{SCE}}$ ), hydrated U(VI) silicate accumulated on the surface. However, the presence of silicate had little influence on the oxidation of  $\text{UO}_2$  to produce an oxidized (altered) surface layer. Note that the concentrations of calcium and silicate used in Santos, et al. (2006a,b) were relatively high (i.e.,  $>0.5 \text{ M Ca}^{2+}$  or  $0.1 \text{ M}$  silicate) to have a significant effect on the anodic dissolution compared to those in this study ( $0.13 \text{ mM Ca}^{2+}$  and  $0.61 \text{ mM}$  silicate).

For the case of 6 percent burnup SIMFUEL, as seen in Figure 3-6, corrosion potentials quickly increased with time and reached 0.1 and 0.06  $\text{V}_{\text{SCE}}$  for the without and with calcium and silicate addition, respectively. These potentials are relatively lower than those of 3 percent SIMFUEL in the amount of average 22 mV. According to the fundamental electrochemical mixed potential



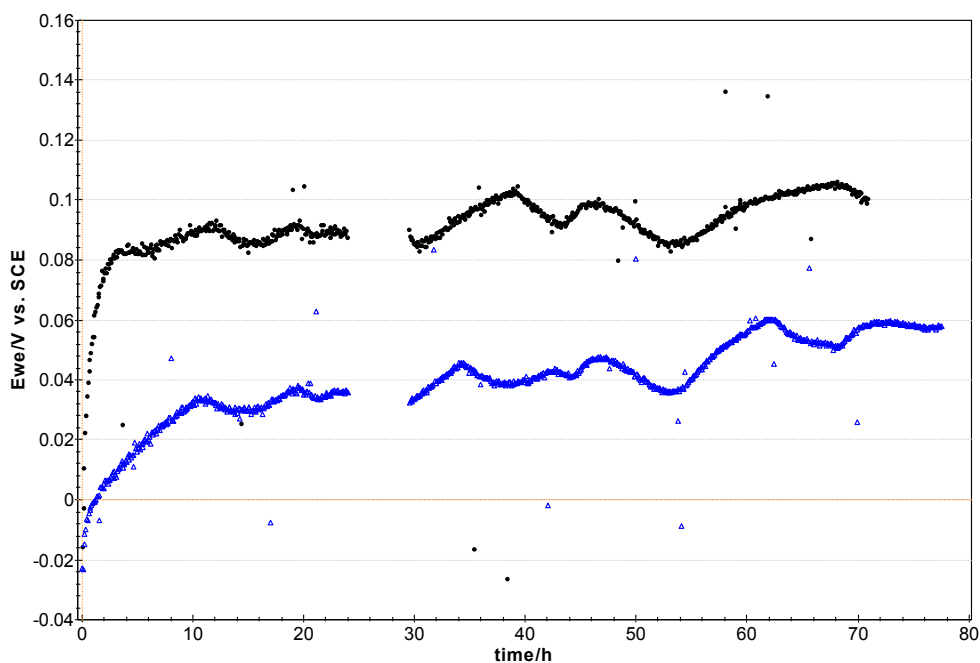
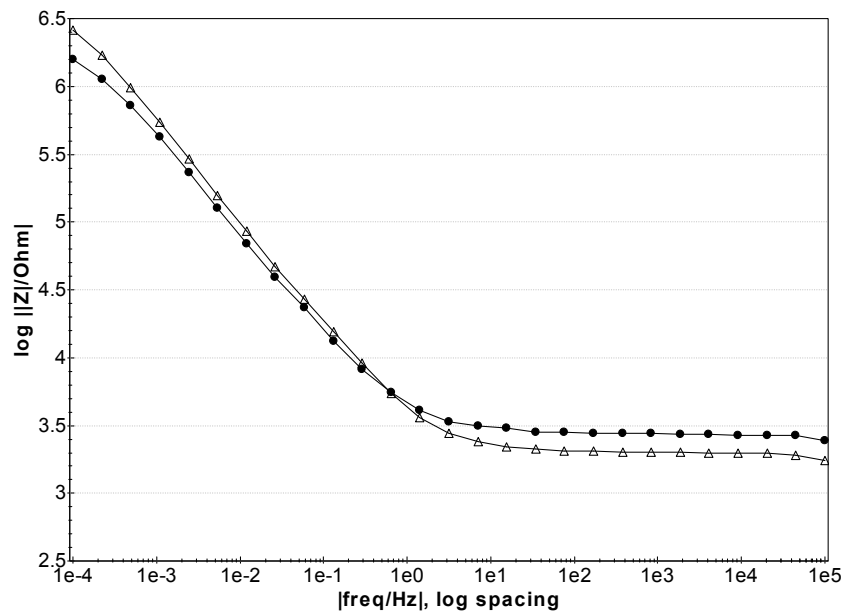


**Figure 3-6. Corrosion Potential Changes of 6 Percent Burnup SIMFUEL Electrode With Time Tested in a Simulated Groundwater Without (●) and With (Δ) Calcium and Silicate Addition at 22 °C [72 °F]**

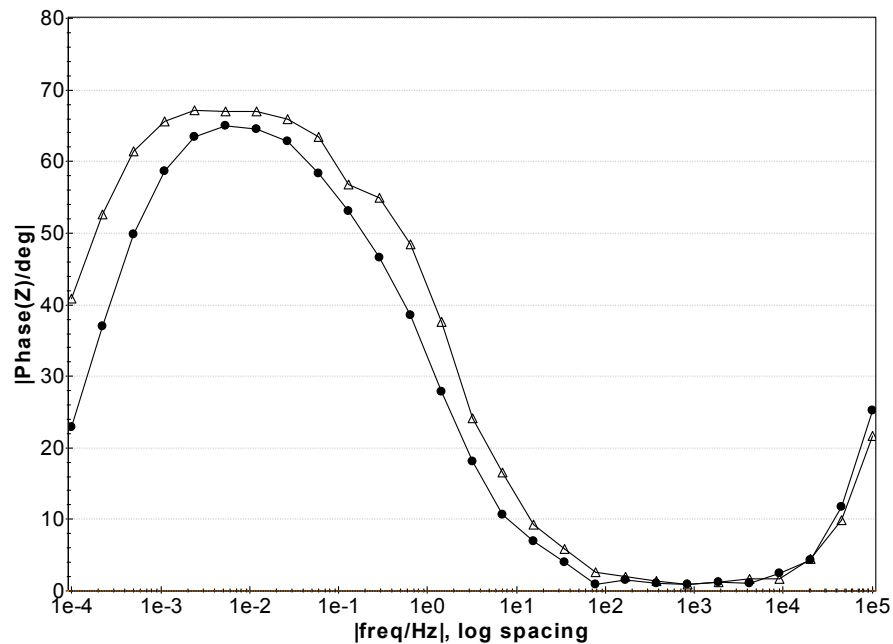
principles, corrosion potential is determined by balancing the anodic oxidation current and the cathodic reduction current. Thus, the lower corrosion potential of 6 percent SIMFUEL could be as a result of either relatively higher anodic dissolution rate from the fuel surface or relatively lower cathodic reduction rate on the fuel surface. Considering relatively smaller grain size and higher heterogeneity of 6 percent SIMFUEL compared to that of the 3 percent SIMFUEL, it is likely that a relatively higher grain boundary area with more precipitates on the 6 percent SIMFUEL surface can lead to a more rapid and higher anodic dissolution rate of 6 percent SIMFUEL. This may be supported by observation of preferential dissolution in the grain boundaries on the SIMFUEL surface (Santos, et al., 2006a). Regarding a cathodic reaction, it was reported that rare-earth dopants such as yttrium, lanthanum, cerium, and neodymium in SIMFUEL (Shoesmith, et al., 1996) or noble metal inclusions such as molybdenum, technetium, ruthenium, rhodium, and palladium in SIMFUEL (Martin, et al., 2008; Broczkowski, et al., 2005) played a role of catalysis in the reduction of oxidants (e.g., dissolved oxygen in the solution), resulting in an increase of cathodic reduction rate. Therefore, it is likely that the lower corrosion potential of the 6 percent SIMFUEL could be a result of a relatively higher anodic dissolution rate compared to the 3 percent SIMFUEL surface.

### 3.2.2 Electrochemical Impedance Spectroscopy

The corrosion of the SIMFUEL surface was characterized using the EIS measured at the corrosion potential. Figure 3-7 shows the Bode plots of the measured impedance spectra of 3 percent burnup SIMFUEL after 24 and 77 hours immersed in a simulated groundwater without calcium and silicate addition at 22 °C [72 °F].



(a) Impedance Versus Frequency



(b) Phase Versus Frequency

**Figure 3-7. Electrochemical Impedance Spectra of 3 Percent Burnup SIMFUEL Measured After 24 (●) and 77 Hours (Δ) Immersion at Corrosion Potential Tested in a Simulated Groundwater Without Calcium and Silicate Addition at 22 °C [72 °F]**

Up to very low frequency range (i.e., 0.0001 Hz), two time constants are apparent: (i) the plateau at a high frequency range (from  $10^4$  Hz up to about 1 Hz) representing the ohmic resistance due to mainly intrinsic electrical resistance of the SIMFUEL pellet and solution resistance and (ii) the linear slope at a relatively low frequency range (i.e., below 1 Hz) representing polarization resistance at the interface between the SIMFUEL surface and solution.

With an increase of immersion time from 24 hours to 77 hours, there is an increase in the impedance modulus,  $|z|$  (i.e., absolute value of the impedance on the y-axis), indicating higher polarization resistance of the SIMFUEL after 77 hours. Corrosion resistance is generally proportional to the polarization resistance (i.e., magnitude of impedance modulus) because the ohmic resistance is negligible (e.g., less than 2.8 kilo-ohms) compared to the polarization resistance (e.g., an order of  $10^6$  ohms). As seen in Figure 3-7(b), compared to the 24-hour curve, there is a tendency to broaden the phase angle curve for the 77 hours in a low frequency range, indicating another time constant is present even if it is not remarkable. This third time constant could be due to a formation of a secondary phase (e.g., schoepite) as is usually observed in similar solutions in the literature (Shoesmith and Sunder, 1998; Shoesmith, et al., 1996; Shoesmith, 2000).

For the impedance spectra of the 3 percent burnup SIMFUEL for the with case (Figure 3-8), the Bode plots were very similar to the without case in terms of impedance modulus and time constant. This result indicates a similar polarization resistance and the same or similar dissolution mechanism for the without case.

For the case of 6 percent SIMFUEL, as seen in Figures 3-9 and 3-10, the shape of the Bode plots was very similar to that of 3 percent SIMFUEL, indicating no changes in the corrosion mechanisms of the 6 percent SIMFUEL. However, 6 percent SIMFUEL exhibited a relatively lower polarization resistance (i.e., impedance modulus) compared to that of 3 percent SIMFUEL for both the without and with cases. Therefore, 6 percent SIMFUEL is expected to have a higher dissolution rate than that of 3 percent SIMFUEL. This expectation is consistent with the observed lower corrosion potential of 6 percent SIMFUEL as discussed previously.

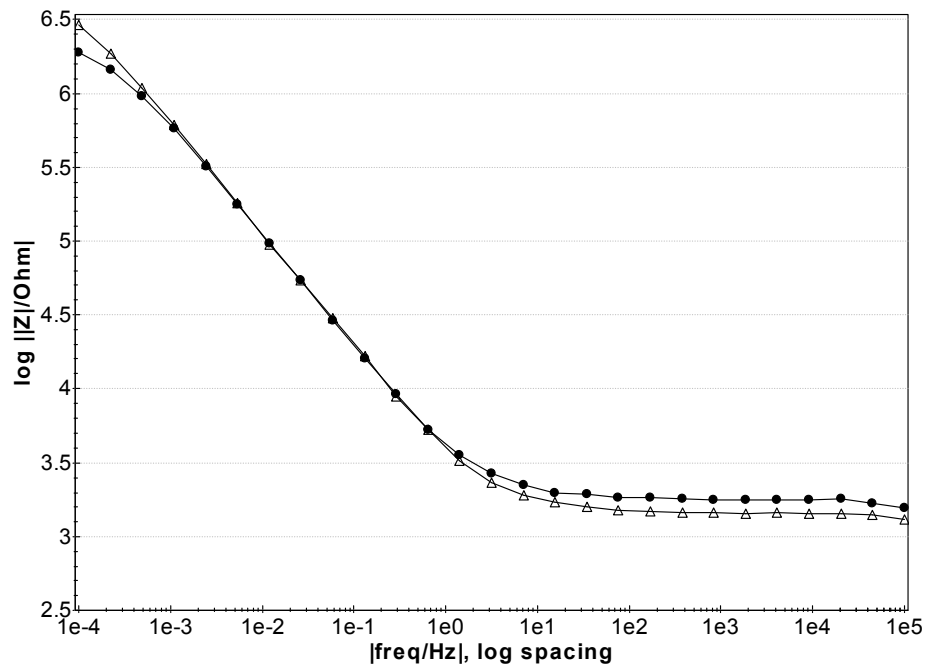
### 3.2.3 Dissolution Rate Estimate

The dissolution (corrosion) rate of SIMFUEL was estimated by fitting the impedance spectra with an appropriate electrical circuit model. As two time constants were apparent within the experiments conducted and the SIMFUEL surface was relatively compact without any clear evidence of crack or porosity as seen in Figures 3-1 and 3-2, a simple Randle circuit was employed consisting of two circuits in series. The first describes the ohmic resistance of the SIMFUEL pellet and solution resistance at high frequency range. The second circuit is related to the SIMFUEL electrode/solution interface and consists of the polarization resistance in parallel connection to the double-layer capacitance at low frequency range. The dissolution rate is calculated from the polarization resistance using the Stern-Geary equation (Stern and Geary, 1957) and Faraday's law, as shown in Eqs. (3-1) and (3-2), respectively

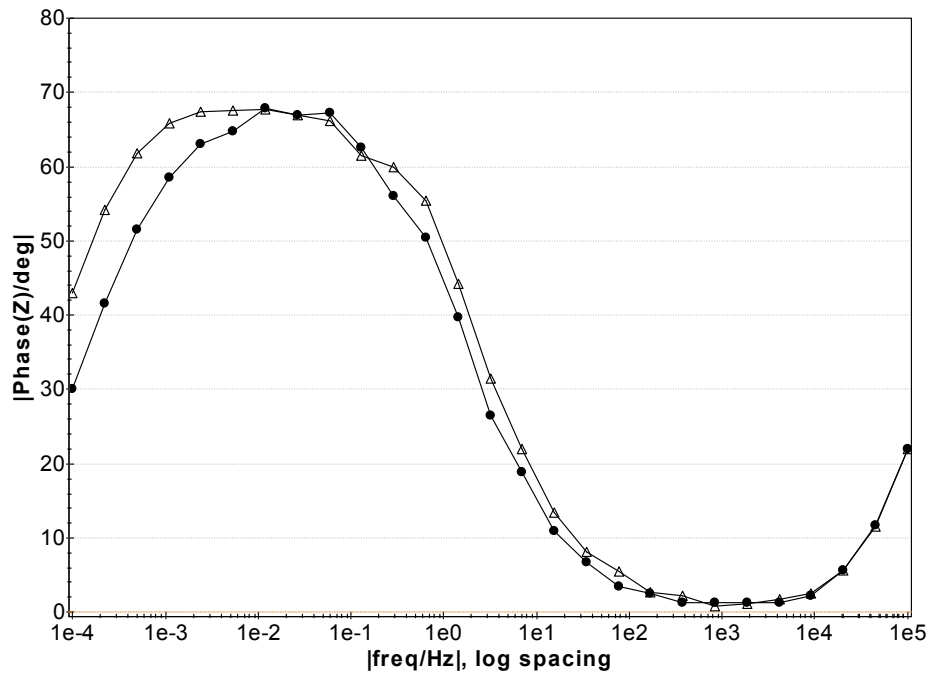
$$i_{corr} = B / R_p \quad (3-1)$$

$$B = b_a \times b_c / [2.303(b_a + b_c)]$$

where  $i_{corr}$ , is corrosion current density;  $R_p$ , is polarization resistance; and  $b_a$  and  $b_c$  are anodic and cathodic Tafel slopes, respectively.

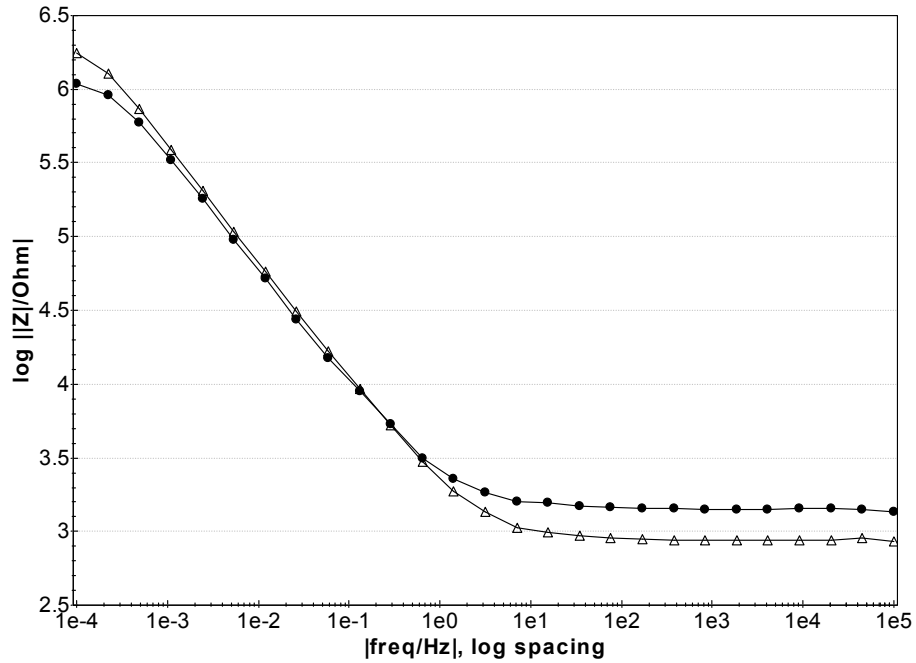


(a) Impedance Versus Frequency

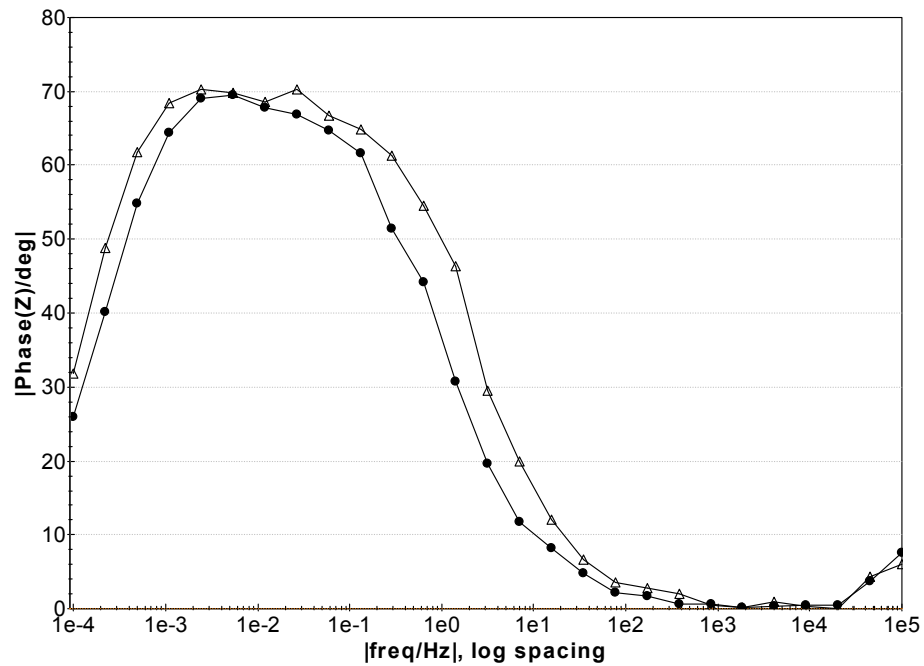


(b) Phase Versus Frequency

**Figure 3-8. Electrochemical Impedance Spectra of 3 Percent Burnup SIMFUEL Measured After 24 (●) and 77 Hours (Δ) Immersion at Corrosion Potential Tested in a Simulated Groundwater With Calcium and Silicate Addition at 22 °C [72 °F]**

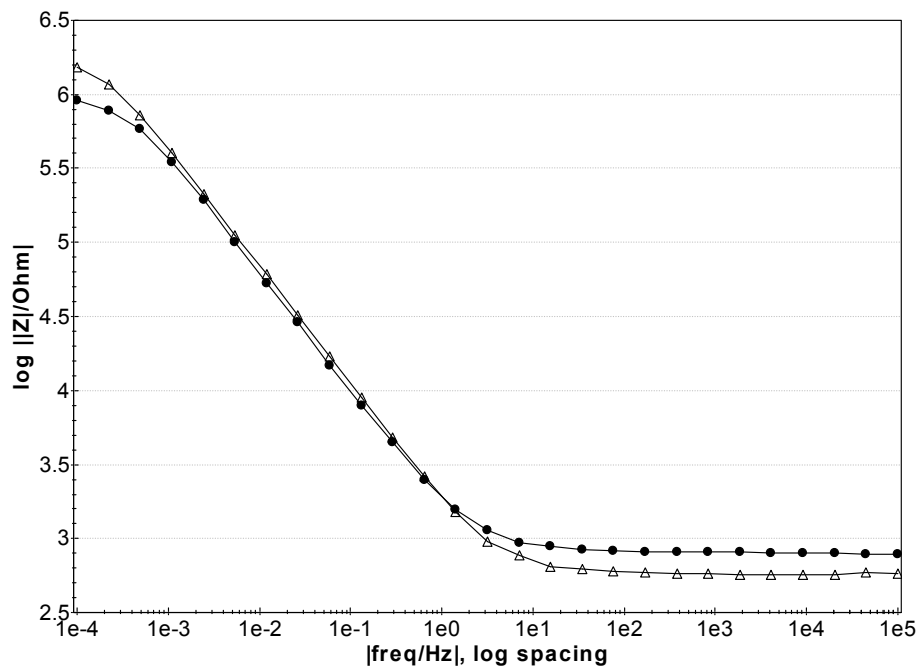


(a) Impedance Versus Frequency

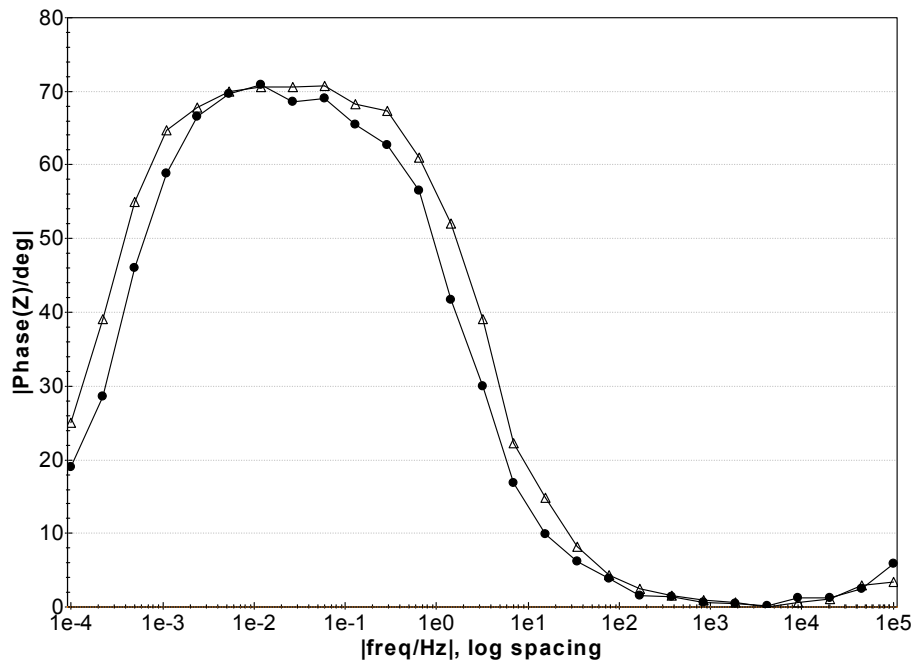


(b) Phase Versus Frequency

**Figure 3-9. Electrochemical Impedance Spectra of 6 Percent Burnup SIMFUEL Measured After 24 (●) and 77 Hours (Δ) Immersion at Corrosion Potential Tested in a Simulated Groundwater Without Calcium and Silicate Addition at 22 °C [72 °F]**



(a) Impedance Versus Frequency



(b) Phase Versus Frequency

**Figure 3-10. Electrochemical Impedance Spectra of 6 Percent Burnup SIMFUEL Measured After 24 (●) and 77 Hours (Δ) Immersion at Corrosion Potential Tested in a Simulated Groundwater With Calcium and Silicate Addition at 22 °C [72 °F]**

The value of the composite Tafel parameter B for uranium dissolution used in this study is selected to be 25 mV based on the literature data (Miserque, et al., 2001; Grambow, et al., 2000).

$$\text{Dissolution (Corrosion) Rate} = K_2 \times i_{\text{corr}} \times EW \quad (3-2)$$

where  $K_2$  is the constant (0.0895 mg cm<sup>2</sup>/μA dm<sup>2</sup> day) and EW, is the equivalent weight for UO<sub>2</sub>.

The equivalent weight of UO<sub>2</sub> used in this study is 33.75 based on 88.15 mass percent of U and 11.85 mass percent of O assuming +6 and -2 valences of U and O, respectively.

Table 3-2 listed the calculated dissolution rates of 3 and 6 percent SIMFUEL tested in simulated groundwater or the in-package chemistry water after 72 hours' immersion. The related parameters are also included in the table. The dissolution rate was calculated based on the geometric surface area of the SIMFUEL surface exposed to solution {i.e., 1.13 cm<sup>2</sup> [ 0.175 in<sup>2</sup> ]}.

Because the Bode plots of the 6 percent SIMFUEL tested in the in-package chemistry water were very similar to those tested in the simulated groundwater for both the without and with cases, the same electrical circuit used for the simulated groundwater was employed to fit the impedance spectra.

For all tested cases, SIMFUEL exhibited very high polarization resistance on the order of 10<sup>6</sup> ohms, indicating that it is highly corrosion resistant. Miserque, et al. (2001) also observed this high resistance. A polarization resistance of 6.8 × 10<sup>6</sup> ohms was reported for the UO<sub>2</sub> pellet tested in 0.1 M KCl (pH = 6) at room temperature. As listed in Table 3-2, the calculated dissolution rates of SIMFUEL range from 1 to 3 mg/m<sup>2</sup>-day under the test conditions in this study. This range of rates is consistent with the reported values summarized in Table 1-1. In particular, as seen in Table 1-1, the dissolution rates of SNF under similar test conditions (i.e., immersion in a simulated groundwater at room temperature) are 0.4 to 3.9 mg/m<sup>2</sup>-day, which are very close to the rates estimated in this study.

In the simulated groundwater tested in this study, the burnup effect on SIMFUEL dissolution rates was consistent. The dissolution rate of 6 percent SIMFUEL is relatively higher than that of 3 percent SIMFUEL for both the without and with cases by a factor of two to three.

Forsyth (1997) reported that the cumulative fractional release of radionuclides such as Cs-137 and Sr-90 of SNF increased with burnup almost linearly up to values of 40–45 MWd/kg U, but afterwards the rates decreased up to 49 MWd/kg U.

The effect of the calcium and silicate addition on the dissolution rate of SIMFUEL was not significant under the conditions tested in this study. This result could be due to very low concentrations of calcium and silicate in this study and/or the masking effect of schoepite formation. Nonetheless, the effect of the calcium and silicate addition did not significantly affect the dissolution rate of SIMFUEL under the conditions tested in this study.

In the in-package chemistry water, the dissolution rate of 6 percent SIMFUEL was slightly lower compared to the simulated groundwater. This result could be due to a lower carbonate concentration in the in-package chemistry water.

<b>Table 3-2. Calculated Dissolution Rates of SIMFUEL Obtained From Impedance Measurements</b>						
	<b>Simulated Groundwater</b>				<b>In-Package Chemistry Water</b>	
SIMFUEL Burnup (at%)	3 Percent		6 Percent		6 Percent	
Ca and Silicate Addition	Without	With	Without	With	Without	With
$R_p$ , Polarization Resistance (Ohms)	$5.76 \times 10^6$	$6.66 \times 10^6$	$2.95 \times 10^6$	$2.20 \times 10^6$	$3.48 \times 10^6$	$3.04 \times 10^6$
$i_{corr}$ , Corrosion Current Density ( $A/cm^2$ )	$3.08 \times 10^{-9}$	$2.66 \times 10^{-9}$	$6.01 \times 10^{-9}$	$8.06 \times 10^{-9}$	$5.10 \times 10^{-9}$	$5.83 \times 10^{-9}$
Dissolution Rate ( $mg/m^2$ -day)	1.15	1.00	2.25	3.01	1.91	2.18

### 3.3 Solution Chemistry Analyses

The measured solution concentrations of barium, chromium, iron, molybdenum, nickel, strontium, zirconium, and uranium are shown in Figure 3-11. The element concentrations plotted in the figure were corrected for the amounts present in the blank solutions. As shown in the figure, the concentration of uranium, which is the dominant element present in the SIMFUEL matrix (see Table 3-1), ranges from  $7.5 \times 10^{-9}$  to  $1.9 \times 10^{-8}$  mol/L. The uranium concentration from the tests that used a 6 percent burnup SIMFUEL is almost twice the uranium concentration from tests that used a 3 percent burnup SIMFUEL. The solution concentration of molybdenum, which is a dominant element in the SIMFUEL grain boundary precipitate, is similar to that of uranium, ranging from  $6.6 \times 10^{-9}$  to  $1.2 \times 10^{-8}$  mol/L. Considering a relatively very small amount of molybdenum is present on the SIMFUEL surface compared to uranium content, as seen in Table 3-1, it is likely that molybdenum could be dissolved preferentially to uranium. The relative mass fraction of molybdenum to uranium is 0.005 and 0.01 for 3 and 6 percent burnup, respectively. The other fission-product-simulating elements, such as barium and zirconium, also have a similar tendency.

Iron, nickel, and chromium occur only as minor elements in the SIMFUEL grain boundary precipitate (see Table 3-1). In spite of their low concentrations in SIMFUEL, iron and nickel generally have high concentrations in the aqueous samples indicating preferential dissolution of iron and nickel. In contrast, the solution concentration of chromium is low. The low concentration of strontium in solution reflects its very low concentration in SIMFUEL (see Table 3-1).

Figure 3-12 shows the calculated fractional release rate for barium, molybdenum, strontium, zirconium, and uranium. The release rate decreases in the order  $Ba > Mo \approx Zr > Sr > U$ . The higher release rates for barium, molybdenum, and zirconium could be due to the preferential dissolution of the precipitate content present in the SIMFUEL matrix (e.g., Zr) and at the grain boundary (e.g., Mo, Ba, and Zr). The relatively low rate of uranium release could be a result of secondary phase formation. As mentioned previously (see Section 3.2.2), there was an indication of possible formation of secondary phases from the impedance spectra after 72 hours' immersion. In the literature, the formation of schoepite was usually observed in similar solutions under an oxidizing condition (Shoesmith, et al., 1996; Santos, et al., 2004; Shoesmith, 2000).



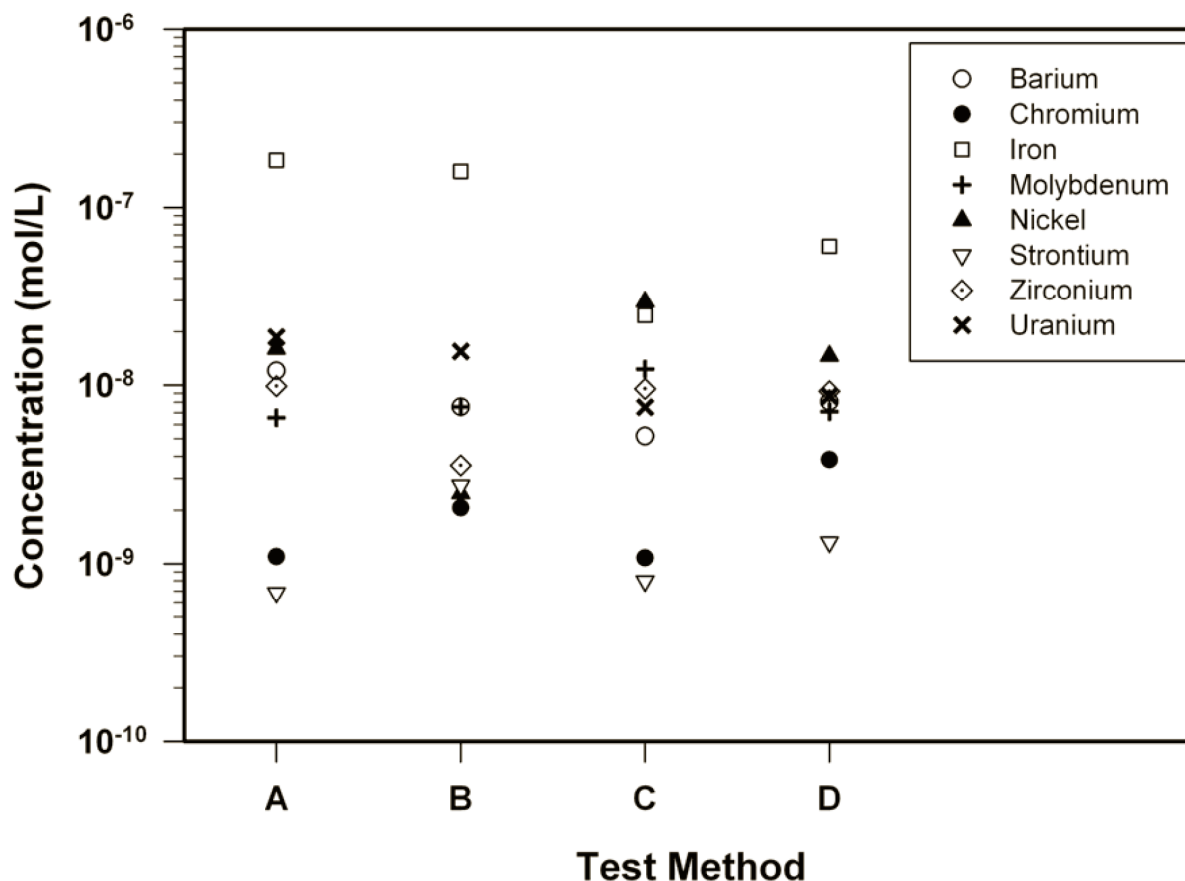


**Figure 3-11. Concentrations of Dissolved Metallic Species in Samples from SIMFUEL Corrosion Test After 3.25 Days at 22 °C [72 °F]. Test Method A: 6 Percent Burnup (With Calcium and Silicate). Test Method B: 6 Percent Burnup (Without Calcium and Silicate). Test Method C: 3 Percent Burnup (With Calcium and Silicate). Test Method D: 3 Percent Burnup (Without Calcium and Silicate).**

The calculated uranium release rates range from 1.0 to 2.6 mg/m<sup>2</sup>-day, which are very close to the rates of 1 to 3 mg/m<sup>2</sup> day determined by impedance measurements after a 77-hour immersion time (see Table 3-2). The calculated uranium release rates suggest that SIMFUEL dissolution is controlled by the uranium dissolution process. In particular, the dependence of release rate on burnup and solution chemistry observed from the solution analysis has the same trend as that determined from the electrochemical impedance measurements. The release rate of strontium is higher than uranium, which is consistent with literature data (Serrano-Purroy, et al., 2009; Röllin, et al., 2001) and has been attributed to fission product migration to the grain boundaries upon irradiation.

The data from the sorption test onto stainless steel disks are presented in Figure 3-13, which shows that uranium and barium concentrations decreased by about 20 percent after immersion of the disks in the test solutions for 21 days. The decrease in uranium and barium concentrations is likely due to sorption onto the stainless steel disks. On the other hand, iron, nickel, and chromium concentrations increased, most likely due to corrosion of the stainless steel disks, which are composed mainly of iron, chromium, and nickel (see Table 2-1). Strontium concentration in solution also increased, but the reason for this increase is not known at this time. The change in molybdenum and zirconium solution concentrations showed

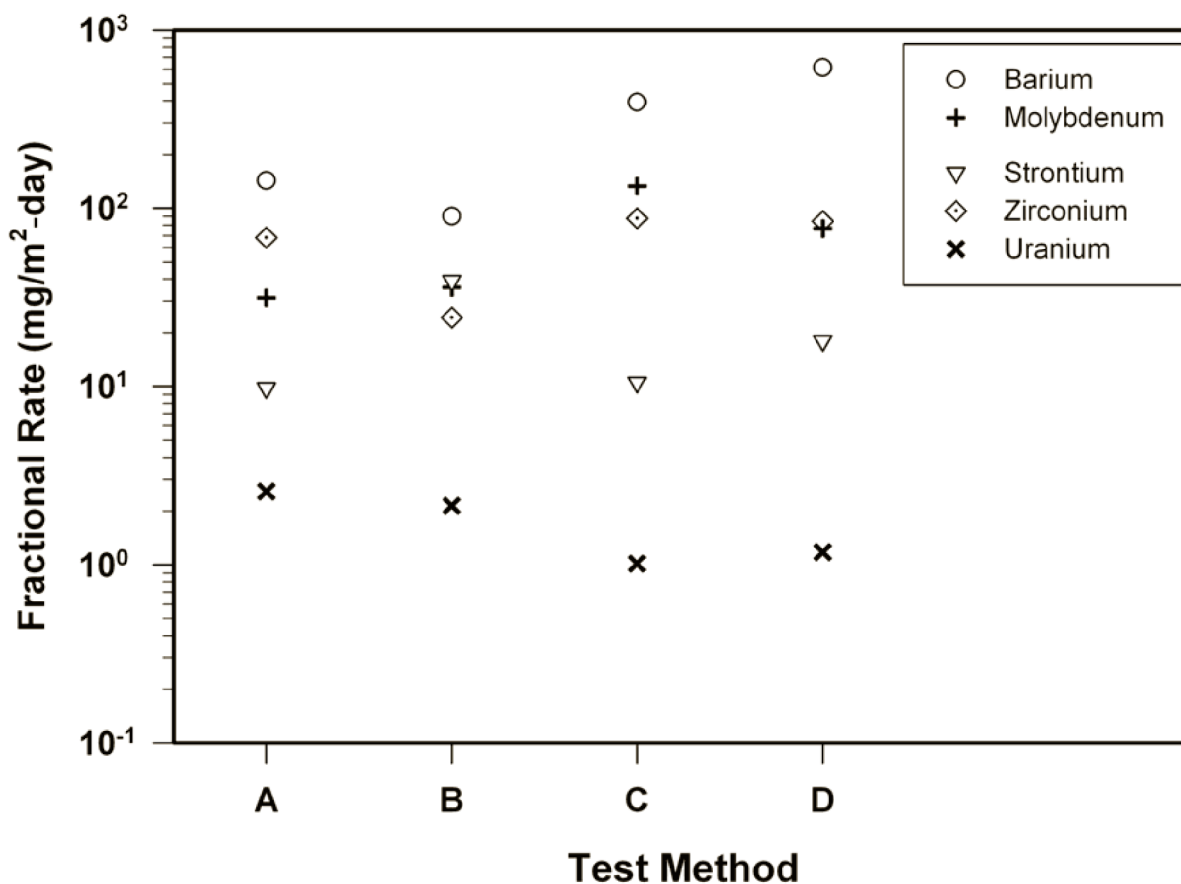


**Figure 3-12. Converted Dissolution Rates of Uranium, Barium, Molybdenum, Strontium, and Zirconium After 3.25 Days of SIMFUEL Corrosion Test at 22 °C [72 °F].**  
**Test Method A: 6 Percent Burnup (With Calcium and Silicate). Test Method B: 6 Percent Burnup (Without Calcium and Silicate). Test Method C: 3 Percent Burnup (With Calcium and Silicate). Test Method D: 3 Percent Burnup (Without Calcium and Silicate).**

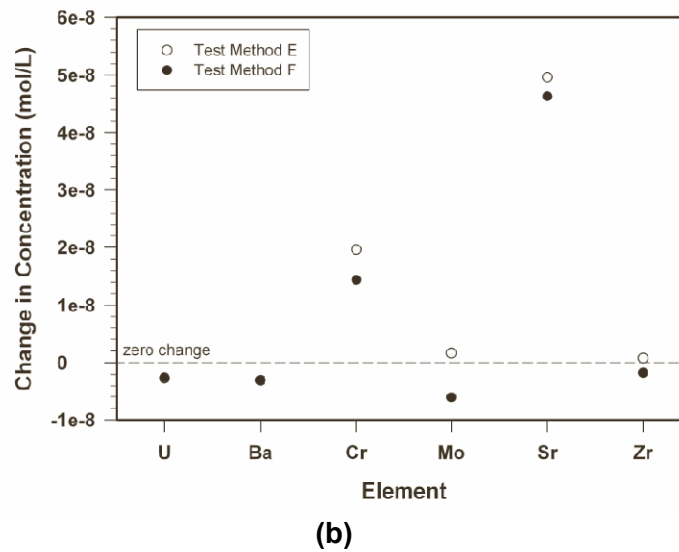
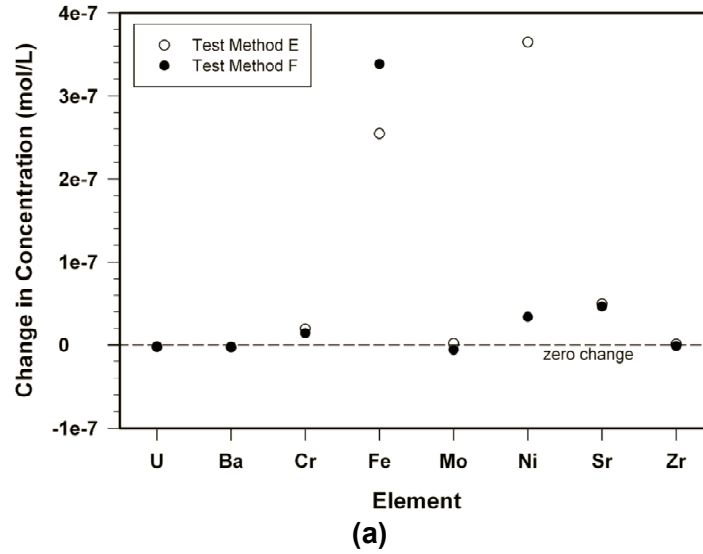


**Figure 3-13. Changes in Aqueous Concentrations of Uranium, Barium, Chromium, Iron, Molybdenum, Nickel, Strontium, and Zirconium After Immersion of Stainless Steel Disk in Test Solutions for 21 Days. Test Method E: Sorption Test Using the Posttest Aqueous Solution From Test Method B. Test Method F: Sorption Test Using the Posttest Aqueous Solution From Test Method D. Iron and Nickel Are Not Plotted in Figure 3-13(b) To Expand the Y-Axis Scale.**

opposite inconsistent trends. The tests that used a 6 percent burnup SIMFUEL showed a decrease in molybdenum and zirconium concentration, whereas the tests that used a 3 percent burnup SIMFUEL showed a slight increase in solution concentration. The reason for this inconsistency is not known at this time.

### 3.4 Thermodynamic Stability of Uranium-Simulated Groundwater System at 22 °C [72 °F]

Figure 3-14 presents the thermodynamic calculation results for a uranium-simulated groundwater system at 22 °C [72 °F] at a concentration of  $10^{-8}$  M for uranium species. In Figure 3-14, uranium can dissolve as  $\text{UO}_2\text{OH}^+$ ,  $\text{UO}_2\text{CO}_3(\text{aq})$ , or  $\text{UO}_2(\text{CO}_3)_2^{2-}$  in weakly acidic to weakly alkaline solutions. With increasing potential, uranium oxide,  $\text{UO}_2$ , can further oxidize to higher oxidation states such as  $\text{UO}_{2.25}$ ,  $\text{UO}_{2.3333}$ , and  $\text{UO}_{2.6667}$ . The alteration of the uranium oxide surface was reported in the literature (Shoesmith, 2000).

With increasing the concentration of uranium species from  $10^{-8}$  to  $10^{-7}$  M as seen in Figure 3-15, schoepite ( $\text{UO}_3 \cdot 2\text{H}_2\text{O}$ ) can form as a stable phase in neutral pH. At the concentration of  $10^{-6}$  M (see Figure 3-16), a region of schoepite is further expanded to a wide range of pH ranging from 6 to 8. Therefore, during the corrosion test conducted in this study, formation of schoepite was very likely. The initial solution pH of simulated groundwater in this study was 8, and the corrosion potentials of SIMFUEL ranged from 0.3 to 0.36  $\text{V}_{\text{SHE}}$ .

Note that there is no stable region for calcium and silicon species under the calculation results, perhaps due to very low initial concentrations of calcium and silicate used in this study, which are not enough to represent as a dominant species any thermodynamically stable species.

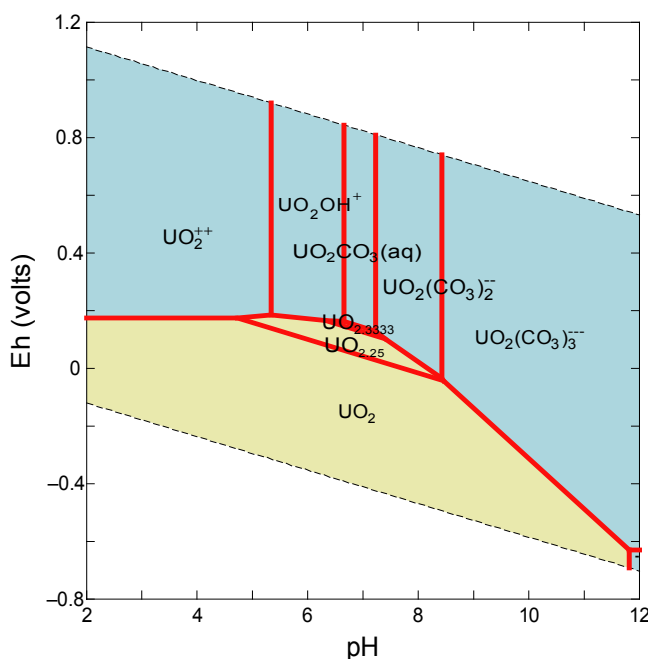


**Figure 3-14. Potential-pH Diagrams for Uranium-Simulated Groundwater Systems at 22 °C [72 °F] at the Concentration of Dissolved Uranium Species of  $10^{-8}$  M**

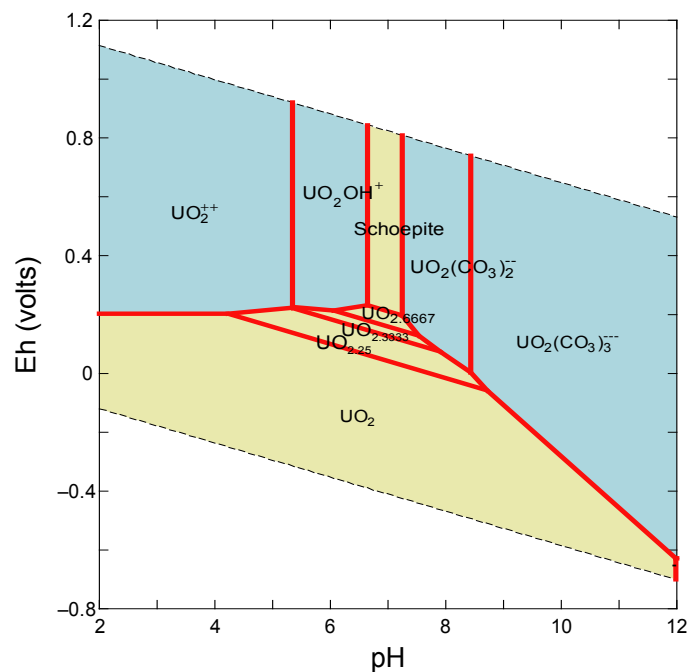


**Figure 3-15. Potential-pH Diagrams for Uranium-Simulated Groundwater Systems at 22 °C [72 °F] at the Concentration of Dissolved Uranium Species of  $10^{-7}$  M**

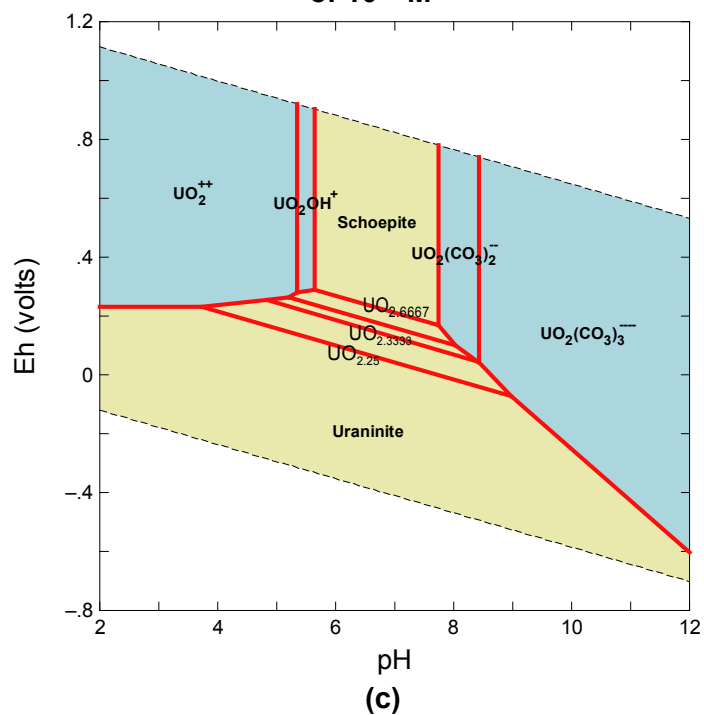


**Figure 3-16. Potential-pH Diagrams for Uranium-Simulated Groundwater Systems At 22 °C [72 °F] at the Concentration of Dissolved Uranium Species of  $10^{-6}$  M**

## 4 CONCLUSIONS

In this report, corrosion behavior of SIMFUEL as an analog material for SNF was evaluated under oxidizing conditions through corrosion tests (electrochemical and non-electrochemical solution analysis) and thermodynamic computation. The main conclusions from this study follow.

- Under test conditions in this study, the measured dissolution rates of 3 and 6 percent burnup SIMFUEL ranged from 1 to 3 mg/m<sup>2</sup> day and a high burnup of SIMFUEL (6 percent) presented a higher dissolution rate than 3 percent burnup SIMFUEL. The range of dissolution rates measured in this study is consistent with the literature data obtained, considering radioactivity decays during the containment period. Compared to accelerated conditions by using relatively high concentrations of carbonate-based solutions, the dissolution rates measured in this study are lower than the rates obtained under accelerated conditions.
- By comparing the dissolution rate measured by electrochemical methods to the uranium release rate measured by solution analysis, it was found that SIMFUEL dissolution is controlled by the uranium dissolution process. The dissolution of other fission product surrogates, such as barium, molybdenum, strontium, and zirconium, were not congruent with uranium.
- The uranium oxide dissolution appeared to be protected by secondary phases such as schoepite that formed on the SIMFUEL surface. The formation of stable schoepite is predicted from the results of thermodynamic stability calculations that may support an observation of increased corrosion resistance with time due to secondary phase formation.
- The effect of calcium and silicate addition on the dissolution rate of SIMFUEL was not significant under the conditions tested in this study. This result could be due to the low concentrations of calcium and silicate used in this study and/or the masking effect of schoepite formed on the SIMFUEL surface.
- Sorption test results showed that the uranium concentrations in the posttest solutions with a stainless steel disk decreased by about 20 percent after 21 days' immersion of stainless steel compared to the concentrations without stainless steel immersed, indicating significant sorption of uranium onto the oxide formed on the stainless steel.
- The electrochemical impedance technique is found to be an effective tool in measuring uranium dissolution rate in real time. This technique can also be used to improve understanding of the uranium dissolution process at the interface between uranium oxide and solution.
- Based on the characterization results of the SIMFUEL microstructure and chemical composition in comparison with other previously reported data for SNF, it is found that SIMFUEL can be used to represent SNF dissolution rate after a long-term containment period when gamma/beta radiation decreases significantly in a repository environment.

## 5 REFERENCES

- Ahn, T. and S. Mohanty. NUREG–1914, “Dissolution Kinetics of Commercial Spent Nuclear Fuels in the Potential Yucca Mountain Repository Environment.” ML 083120074. Washington, DC: U.S. Nuclear Regulatory Commission. 2008.  
<www.nrc.gov/reading-rm/adams.html> (1 March 2009).
- Bottomley, P.D.W., D.-H. Wegen, and M. Coquerelle. “Construction of an Electrode for Irradiated  $\text{UO}_2$  Fuel and Preliminary Results Concerning its Use in Aqueous Solution.” *Journal of Nuclear Materials*. Vol. 238. pp. 23–37. 1996.
- Broczkowski, M.E., J.J. Noel., and D.W. Shoesmith. “The Inhibiting Effects of Hydrogen on the Corrosion of Uranium Dioxide Under Nuclear Waste Disposal Conditions.” *Journal of Nuclear Materials*. Vol. 346. pp. 16–23. 2005.
- Bruno, J., I. Casas, and A. Sandino. “Static and Dynamic SIMFUEL Dissolution Studies Under Oxidic Condition.” *Journal of Nuclear Materials*. Vol. 190. pp. 61–69. 1992.
- Choi, J.W., R.J. McEachen, P. Taylor, and D.D. Wood. “The Effect of Fission Products on the Rate of  $\text{U}_3\text{O}_8$  Formation in SIMFUEL Oxidized in Air at 250 °C.” *Journal of Nuclear Materials*. Vol. 230. pp. 250–258. 1996.
- Cunnane, J., K. Czerwinski, B. Ebert, D. Kolman, E. Mausolf, and M. Williamson. “Waste Form Testing Protocols: Alloys.” Savannah River National Laboratory, ASTM C26.07 & C26.13 Workshop, January 27, 2010. San Antonio, Texas: ASTM. 2010.
- Ebert, W.L., M.A. Lewis, T.L. Barber, and S.G. Johnson. “Accounting for EBR-II Metallic Waste Form Degradation in TSPA.” Symposium Proceedings Volume 757. Warrendale, Pennsylvania: Material Research Society. pp. 71–80. 2003.
- Engelhardt, J., F. Feldmainer, M. Laske, and G. Marx. “Impedance Measurements on  $\text{UO}_2=x$  in Saturated NaCl Solutions.” *Journal of Nuclear Materials*. Vol. 238. pp. 104–109. 1996.
- Ferry, C., et al. “Synthesis on the Spent Fuel Long Term Evolution.” CEA–R–6084. Saclay, France: COMMISSARIAT À L’ÉNERGIE ATOMIQUE. 2005.
- Finn, P.A., et al. “Yucca Mountain Project—Argonne National Laboratory: Annual Progress Report, FY 1997.” ANL–98/12. Argonne, Illinois: Argonne National Laboratory. 1998.
- Forsyth, R. “An Evaluation of Results From the Experimental Programmed Performed in the Studsvik Hot Cell Laboratory.” SKB TR 97-25. Stockholm, Sweden: Swedish Nuclear Fuel and Waste Management Company. 1997.
- Grambow, B. et al. “Source Term for Performance Assessment of Spent Fuel as a Waste Form.” European Commission, Nuclear Science and Technology. EUR 19140. Belgium: European Communities. 2000.
- Ishii, B. and Y. Seki. “Microstructure of Irradiated Uranium Dioxide.” *Journal of Nuclear Science and Technology*. Vol. 4, No. 3. pp. 143–148. 1967.

- Johnson, S.G., D.D. Keiser, S.M. Frank, T. DiSanto, A.R. Warren, and M. Noy. "Leaching Characteristics of the Metal Waste Form From the Electrometallurgical Treatment Process: Product Consistency Testing." Warrendale, PA: Material Research Society. Symposium Proceeding Volume 608. pp. 589–594. 2000.
- Lucuta, P.G., H.J. Matzke, and R.A. Verrall. "Thermal Conductivity of Hyperstoichiometric SIMFUEL." *Journal of Nuclear Materials*. Vol. 223. pp. 51–60. 1995.
- Lucuta, P.G., R.A. Verrall, H.J. Matzke, and B.J. Palmer. "Microstructural Features of SIMFUEL–Simulated High-Burnup  $\text{UO}_2$ -Based Nuclear Fuel." *Journal of Nuclear Materials*. Vol. 178. pp. 48–60. 1991.
- Martin, T., S. Nilson, and M. Johnson. "On the Effects of Fission Product Noble Metal Inclusions on the Kinetics of Radiation Induced Dissolution of Spent Nuclear Fuel." *Journal of Nuclear Materials*. Vol. 378. pp. 55–59. 2008.
- Miserque, F., T. Gouder, D.H. Wegen, and P.D.W. Bottomley. "Use of  $\text{UO}_2$  Films Electrochemical Studies." *Journal of Nuclear Materials*. Vol. 298. pp. 280–290. 2001.
- Park, G.I., J.W. Lee, Y.W. Lee, and L.C. Song. "Effect of Impurities on the Microstructure of DUPIC Fuel Pellets Using the SIMFUEL Technique." *Nuclear Engineering and Technology*. Vol. 40, No. 3. pp. 191–198. 2008.
- Rondinella, V. and H.J. Matzke. "Leaching of SIMFUEL in Simulated Granite Water Comparison to Results in Demineralized Water." *Journal of Nuclear Materials*. Vol. 238. pp. 44–57. 1996.
- Rondinella, V. and T. Wiss. "The Shigh Burn-Up Structure in Nuclear Fuel." *Materials Today*. Vol. 13, No. 12. pp. 24–32. 2010.
- Röllin, S., K. Spahiu, and U.-B. Eklund. "Determination of Dissolution Rates of Spent Fuel in Carbonate Solutions Under Different Redox Conditions With a Flow-Through Experiment." *Journal of Nuclear Materials*. Vol. 297. pp. 231–243. 2001.
- Sandia National Laboratory. "In-Package Chemistry Abstraction." ANL–EBS–MD–000037. Rev 04 ADD 01 CAN 01 ERD 1. Las Vegas, Nevada: Sandia National Laboratories. 2007.
- Santos, B.G., J.J. Noel, and D.W. Shoesmith. "The Influence of Calcium Ions on the Development of Acidity in Corrosion Product Deposits on SIMFUEL,  $\text{UO}_2$ ." *Journal of Nuclear Materials*. Vol. 350. pp. 320–331. 2006a.
- Santos, B.G., J.J. Noel, and D.W. Shoesmith. "The Influence of Silicate on the Development of Acidity in Corrosion Product Deposits on SIMFUEL ( $\text{UO}_2$ )." *Corrosion Science*. Vol. 48. pp. 3,852–3,868. 2006b.
- Santos, B.G., H.W. Nesbitt, J.J. Noel, and D.W. Shoesmith. "X-Ray Photoelectron Spectroscopy Study of Anodically Oxidized SIMFUEL Surfaces." *Electrochimica Acta*. Vol. 49. pp. 1,863–1,873. 2004.
- Serrano-Purroy, D., F. Clarens, J.-P. Glatz, D. Wegen, B. Christiansen, J. de Pablo, J. Gimenez, I. Casa, and A. Martinez-Esparza. "Leaching of 53 MW/d kg U Spent Fuel Nuclear Fuel in a Flow-Through Reactor." *Radiochimica Acta*. Vol. 97. pp. 491–496. 2009.



Shoesmith, D.W. "Fuel Corrosion Processes Under Waste Disposal Conditions." *Journal of Nuclear Materials*. Vol. 282. pp. 1–31. 2000.

Shoesmith, D.W. and S. Sunder. "Validation of an Electrochemical Model for the Oxidative Dissolution of Used CANDU Fuel." *Journal of Nuclear Materials*. Vol. 257. pp. 89–98. 1998.

Shoesmith, D.W., S. Sunder, M.G. Bailey, and N.H. Miller. "Corrosion of Used Nuclear Fuel in Aqueous Perchlorate and Carbonate Solutions." *Journal of Nuclear Materials*. Vol. 227. pp. 287–299. 1996.

Stern, M. and A.L. Geary. "Electrochemical Polarization: 1. A Theoretical Analysis of the Shape of Polarization Curves." *Journal of the Electrochemical Society*. Vol. 104, No 1. pp. 56–63. 1957.

Wilson, C.N. and W.J. Gray. "Measurement of Soluble Nuclide Dissolution Rates from Spent Fuel." Symposium Proceedings Volume 176. Warrendale, Pennsylvania: Material Research Society. pp. 489–498. 1990.